2014

Self-Assembly of Peptides to Nanostructures

Dindyal Mandal

Amir Nasrolahi Shirazi
University of Rhode Island

Keykavous Parang
University of Rhode Island, kparang@uri.edu

Citation/Publisher Attribution

Mandal, D., Shirazi, A. N., & Parang, K. (2014). Self-assembly of peptides to nanostructures. *Organic & Biomolecular Chemistry,* 12, 1-57. doi: 10.1039/C4OB00447G
Available at: http://dx.doi.org/10.1039/C4OB00447G

Self-Assembly of Peptides to Nanostructures

Dindyal Mandal,[a,*] Amir Nasrolahi Shirazi,[b,c] and Keykavous Parang[b,c,*]

[a]*School of Biotechnology, KIIT University, Bhubaneswar, Orissa, India*

[b]*Department of Biomedical and Pharmaceutical Sciences, College of Pharmacy, University of Rhode Island, Kingston, Rhode Island 02881, United States*

[c]*School of Pharmacy, Chapman University, Orange, California 92866, United States*

***Corresponding authors.** 7 Greenhouse Road, Department of Biomedical and Pharmaceutical Sciences, College of Pharmacy, University of Rhode Island, Kingston, Rhode Island, 02881, USA; Tel.: +1-401-874-4471; Fax: +1-401-874-5787; E-mail address: kparang@uri.edu,

ddmandal@gmail.com

Abstract

The formation of well-ordered nanostructures through self-assembly of diverse organic and inorganic building blocks has drawn much attention owing to their potential applications in biology and chemistry. Among all organic building blocks, peptides are one of the most promising platforms due to their biocompatibility, chemical diversity, and resemblance with proteins. Inspired from the protein assembly in biological systems, various self-assembled peptide structures have been constructed using several amino acids and sequences. This review focuses on this emerging area, the recent advances in peptide self-assembly, and formation of different nanostructures, such as tubular, fibers, vesicles, spherical, and rod coil structures. While different peptide nanostructures are discovered, potential applications will be explored in drug delivery, tissue engineering, wound healing, and surfactants.

1. Introduction

Nanometer-sized structures have attracted major attention owing to their potential for diverse applications ranging from nanotechnology to biotechnology. In biological systems, proteins, DNA, cellular organelles, and microorganisms are submicron sized objects. Thus, they can be considered as 'biological nanostructures' when compared to synthetic nanostructures.

Self-assembly is a spontaneous process of organization of chaotic molecular units into ordered structures as a result of intramolecular/intermolecular interactions.[1] The process of assembly is controlled by the balance of attractive/repulsive forces within and between molecules. The generation of many biological nanostructures occurs through the self-assembly process, such as DNA double helix formation through hydrogen bonding interactions between nucleotide bases, protein's tertiary or quaternary structure through folding of a polypeptide chain, and the formation of cell membranes upon self-assembly of phospholipids. The most straightforward and extensively known self-assembled structure in a biological system is the lipid membrane structure. The cell membrane consists of lipid bilayers that are arranged in such a way that their hydrocarbon tails face one another to make a hydrophobic bilayer while their hydrophilic head groups are exposed to aqueous solutions on each side of the membrane.

The self-assembly process is mediated through noncovalent interactions including van der Waals, electrostatic, hydrogen bonding, and stacking interactions. The fabrication of new materials using natural building blocks, such as phospholipids, oligosaccharides, oligonucleotides, proteins, and peptides, has become a subject of major interest.[2] Among them, peptides have drawn significant attention due to their simple structure, relative chemical and physical stability, diversity in sequences and shapes, and feasibility to synthesize in large amounts. In addition, peptides have

become known as immensely useful building blocks for creating self-assembled nanostructures in medical applications due to their intrinsic biocompatibility and biodegradability.

Proteins and peptides are made up of 20 natural L-amino acids. All of the natural amino acids are chiral in nature except glycine and contain carboxylic acid and amino groups. The only difference in their structure is in the side chain groups attached to the chiral carbon. Amino acids as building blocks of peptides have various physicochemical properties, because of variety in charge, hydrophobicity, size, and polarity in side chains. The number, type, and sequence of amino acids can be manipulated to design self-assembled peptides. Depending upon the amino acid sequence, the peptide can form different structures. Many human medical disorders are associated with polypeptide self-assembly into amyloid fibrils.[3]

The versatility of the peptides, in conjunction with their ability to form specific secondary structures, provides a unique platform for the design of nanomaterials with controllable structural features. A number of peptide-based building blocks, such as cyclic peptides, amphiphilic peptides, copolypeptides, surfactant-like oligopeptides, dendritic peptides, and aromatic dipeptides, have been designed and developed for generating supramolecular structures and the exploration of their possible applications in biology and nanotechnology. Key advantages of self-assembled peptides relative to conventional structures include biocompatibility, biodegradability, and versatility.

Self-assembled peptide nanostructures have demonstrated considerable potential as biomaterials[4] and use for carrier-mediated drug delivery, tissue engineering, antimicrobial agents, imaging tools, energy storage, biomineralization, and membrane protein stabilization.[5] Thus, the self-assembly properties of peptides have been exploited for generating bio-inspired nanostructures, including nanotubes, nanofibers, nanospheres, nanobelts, and hydrogels.[6]

Herein, we review representative examples and highlights of peptide nanostructures, such as tubular, fibers, ribbons, vesicles, spherical structures, and rod coil structures. A comprehensive review of all self-assembled peptide nanostructures is beyond the scope of this manuscript. We apologize that many excellent works were not included here. Table 1 summarizes the sequences of the peptides and the corresponding formed nanostructures discussed in this review.

2. Peptide Nanostructures

2.1. Tubular Nanostructures

Nanotubes are nanometer size tube-like structures. They are elongated nanostructures which have definite inner hole. Nanotubes are particularly attractive because of their potential applications in biology, chemistry, and physics, such as chemotherapy, drug delivery, catalysis, molecular separation, optics, and electronics.[7] Over the past few decades, researchers have made significant progress in covalently bonded nanostructures. Currently, noncovalent nanotubes have become subjects of major interest due to their significant advantages including facile synthesis, self-organization, control in diameter size, and high efficiency. A number of protocols have been reported for the preparation of the noncovalently self-assembled nanotubes using different structures including hollow bundles of rod-like units, helical structures, and stacked rings. It is generally known that the simplest peptide block for the self-assembly is diphenylalanine peptide (L-Phe-L-Phe, FF),[8] which forms a tubular structure with a long persistence length (~ 100 μm). The self-assembly is mediated through hydrogen bonding as well as π–π stacking of aromatic residues. Other tubular structures include cyclic peptide and peptide amphiphile nanotubes.

2.1.1. Cyclic Peptide Nanotubes

The self-assembled cyclic peptide nanotubes formed by stacking of peptides and stabilization by hydrogen bonds have attracted major interest because of the ease to change their structural and functional properties. For this kind of self-assembly, peptides can adopt particular orientation, where amino acid side chains are directed toward outward whiled the carbonyl and the amino groups of the peptide backbone are directed perpendicular to the ring and participate in intermolecular hydrogen bonding.

The pioneer work on cyclic peptide nanotubular structures was carried out by Ghadiri and co-workers.[9a] They demonstrated a new class of organic nanotubes based on rationally designed of heterochiral cyclic peptides. These peptides formed extended β-sheet-like structures, and stacked on top of each other to form hollow and extended cylinders.[9] The peptide nanotubes were formed using the sequence: *cyclo*[(D-Ala-Glu-D-Ala-Gln)$_2$]. The investigators used alternating D- and L-amino acids in making the cyclic heterochiral octapeptide that generated a planar ring and self-assembled through hydrogen bonding to form nanotube structures with a specific diameter. The self-assembly was triggered in acidic environment and generated nanotube structures through hydrogen bond interactions of ring-shaped peptides subunits. They hypothesized that cyclic peptide having an even number of alternating D-and L-amino acids could adopt a low-energy ring shaped flat conformation. All backbone peptide amide groups became orientated perpendicular to the plane of the structure and participate in backbone-backbone intermolecular hydrogen bonding to generate an adjacent antiparallel β-sheet structure (Figure 1). Thus, controlled acidification of alkaline peptide solution triggered the spontaneous self-assembly of peptide subunits into rod-shaped crystals, which was an organized collection of hundreds of tightly packed nanotubes. Intersubunit hydrogen bonding provided the main driving force in the assembly process. In

contrast, ring stacking is not favorable at alkaline pH, due to the repulsive intermolecular interactions between the negatively charged carboxylate side chains of glutamate. The internal diameter of the nanotubes ranged between 7-8 Å and was controlled by changing the number of amino acids in the peptide sequence.[10]

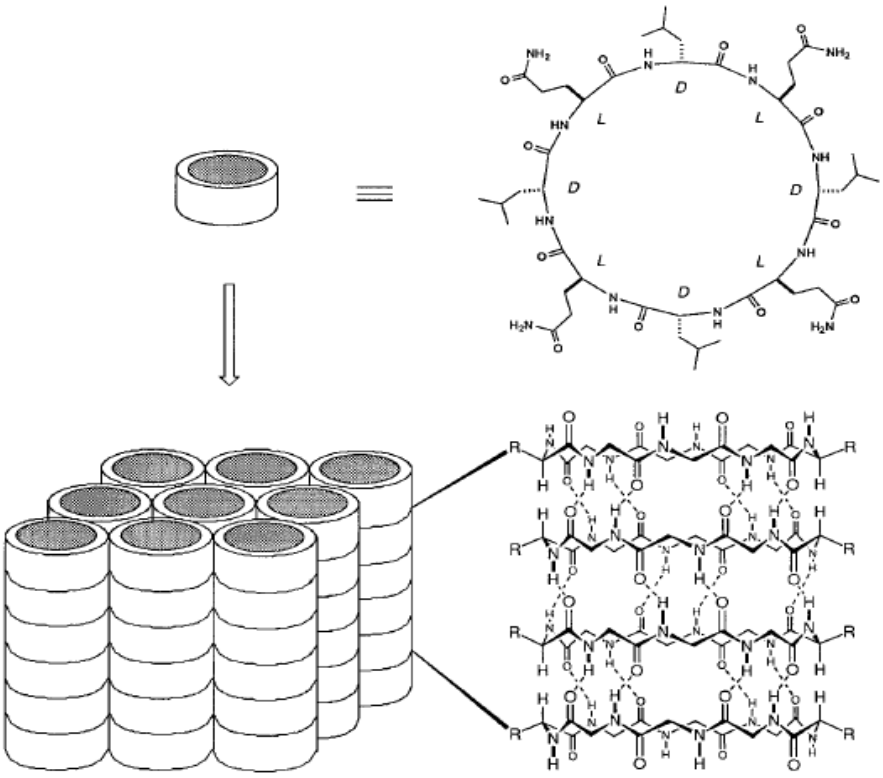

Figure 1. Cyclic peptide structures with alternating D- and L-amino acids adopted flat ring-shaped conformations and assembled into ordered parallel arrays of solid-state nanotubes. The illustration emphasizes the antiparallel ring stacking and the presence of extensive hydrogen-bonding interactions between subunits (for clarity most side chains are omitted). Reprinted with permission from ref. 10. Copyright 2013 American Chemical Society.

Various applications of these peptide nanotubes have been explored in diverse fields. The structural features of these cyclic peptides were very unique. When they were placed in such a

condition that formed hydrogen bonding, for example, adsorption onto lipid membranes, they stacked to form hollow, β-sheet like tubular structures. The authors suggested that rationally designed cyclic D,L-α-peptides could potentially self-assemble in bacterial membranes and exhibit antibacterial activity by increasing the membrane permeability.[11] These cyclic peptides decorated with suitable hydrophobic surface residues formed transmembrane channel structures by spontaneous self-assembly on inclusion of an ample concentration of the peptide monomer in lipid bilayers. They further suggested that not only the hydrophobic nature of the channel-forming peptide was a major factor, but also the peptide played a part in extended hydrogen-bonded stacking interactions to construct long channel structures to wrap the lipid bilayer. Ghadiri et al proposed that the transmembrane channel structures with larger pore diameters could have potential application in molecular transport across lipid bilayers and can be used as a delivery tool into living cells in antisense and gene therapy applications.[9b]

Another cyclic peptide that was reported to self-assemble into tubular structures was the Lanreotide octapeptide, which was synthesized as a growth hormone inhibitor.[12] Lanreotide was shown to self-assemble into nanotubes of viral capsid-like dimension. The nanotube walls were composed of helical filaments that were formed by self-assembly of peptide dimer building blocks to antiparallel β-sheets through an alternating pattern of the aromatic amino acid and aliphatic residues.

2.1.2. Peptide Amphiphile (PA) Nanotubes

Some nanotubular structures were also formed by self-assembly of peptide amphiphiles (PAs).[13] PAs represent a simple category of the designed self-assembling peptides bearing the lipid or surfactant characteristics. They possess a hydrophobic tail and a hydrophilic head. The tails of

PAs are normally composed of nonpolar amino acid residues (G, A, V, I, L, P and F). The tails also can be made of hydrocarbon chains or combination of the hydrocarbon chain and nonpolar amino acids. Positively charged amino acids (H, K, and R) and/or negatively charged residues (D and E) have been found as appropriate to be used in heads. Glycine rich amphiphilic peptide G_nD_2–OH (where n= 4, 6, 8, 10) generated nanotubular structures with two dimensions, one with 40-80 nm and another in the order of 100-200 nm.[14] Molecular modeling studies revealed that peptides formed bilayer structures to confiscate the glycine chains from the aqueous system. Nevertheless, unlike lipids, peptides formed hydrogen bonds with one another on the backbone. The glycines were filled inside of the bilayer away from water and the aspartic acids were exposed to water, similar to other surfactants (Figure 2).

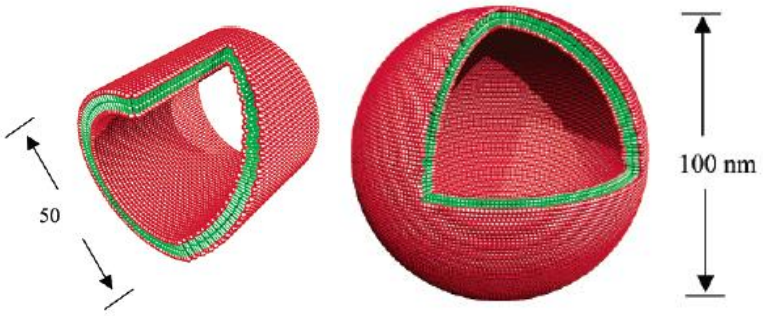

Figure 2. Molecular modeling of cut-away structures formed from the peptides with negatively charged heads and glycine tail. Left picture shows peptide nanotube with an area sliced away. Right picture exhibits a peptide nanovesicle. Color code: red, negatively charged aspartic acid heads; green, nonpolar glycine tail. The modeled dimension is 50-100 nm in diameter. Reprinted with permission from ref. 14. Copyright 2013 American Chemical Society.

Interestingly, peptides containing alanine and valine tails have been found to form more stable structures than those of glycine, isoleucine, and leucine. Peptides containing valine, Ac-V_6D-OH formed nanotube as well as nanovesicles. Tubular structures were found in self-assembly of other PAs, such as trifluoroacetate salt of A_6K and I_3K (Ac-I_3K-NH_2).[15a] The diameter of nanotube formed by A_6K peptide was found to be 25-30 nm, whereas the diameter of nanotubes formed by shorter peptide, I_3K was about 10 nm and lengths over 5 μm. The formation of nanostructures from the short peptide clearly indicates that the balances between the peptide sequence and the size of hydrophobic residues controls the amphiphilicity of a peptide. Then, FTIR and solid sate NMR (SSNMR) spectroscopy was used to elucidate the molecular architecture of the peptide nanotube formed by A_6K.[15b] Qualitative information from FTIR indicated that antiparallel β-strands aligned perpendicular to the nanotube axis. SSNMR technique revealed the tilt angle of the peptide hydrogen bonding axis within the nanotube framework. This class of peptide surfactant exhibited properties similar to those of common surfactants, such as *n*-dodecyl-β-D-maltoside (DM) and octyl-D-glucoside (OG). The potential applications of these peptides were investigated by using A_6D as a model peptide surfactant in the stabilization of membrane protein, such as G protein-coupled receptor bovine rhodopsin.[15c] A_6D not only showed efficiency in stabilizing the membrane protein in the presence of lipid and other common surfactants, but also it can be used as stabilizer alone under thermal denaturation conditions without any common surfactants.

Sometimes molecular geometry also affects the formation of nanostructures. For example, cone-shaped PA, Ac-GAVILRR-NH_2, which has a hydrophobic tail with increasing hydrophobicity and a large cationic head group composed of two arginine residues led to the formation of the simultaneous shapes of nanosphere and nano-doughnut structures (Figure 3).[16]

The outer and inner diameters of the doughnut-shaped structures were around 110 nm and 25 nm, respectively. Self-assembly pathway leading to the pattern of doughnut-shaped nanostructures was probably through fusion or elongation of short spherical micelles that merged side by side to form that nanostructures.[17]

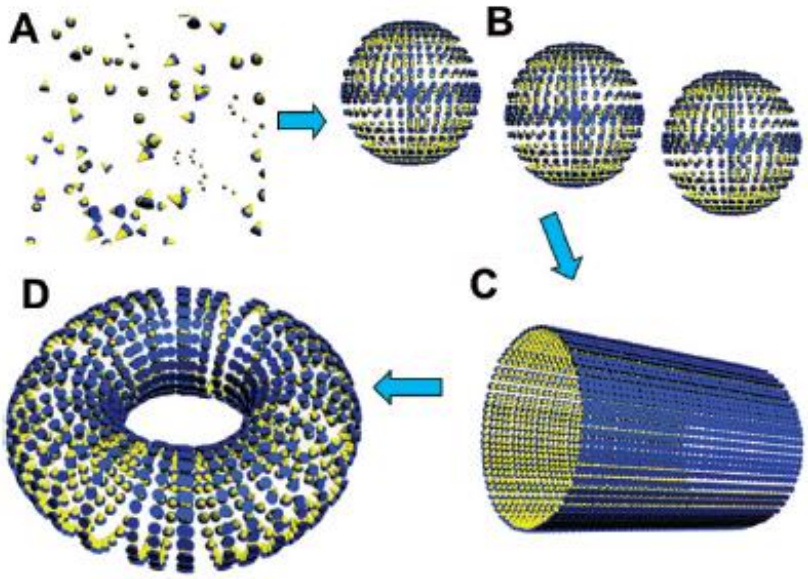

Figure 3. Proposed plausible self-assembly process of the nanodoghnut structure. (A) Randomly oriented and distributed peptides at low concentration; (B) Micelle formation above the critical aggregation concentration (CAC); (C) Fusion or elongation of the micelles for the formation of a nanopipe; (D) Bending of the nanopipe for the formation of a nanodoughnut structure. Reprinted with permission from ref. 16. Copyright 2013 American Chemical Society.

Cone-shaped peptide amphiphiles Ac-$A_2V_2L_3WE_{2/7}$–OH that were produced recombinantly from the bacterial culture,[18] formed nano-vesicles with radius size around 60 nm.

Self-assembly of this peptide started at pH 5.0. This pH triggered self-assembly could be particularly useful in drug delivery applications.

Effect of molecular structure was found in the self-assembly of the series of PAs, such as A_mK (where m = 3, 6 and 9). These peptides showed different shapes and size with increasing hydrophobic tail length. A_3K peptide aggregated at higher concentration compared to A_6K and A_9K, probably due to its weak hydrophobicity. A_3K formed unstable peptide sheet stacks. In contrast, A_6K formed long nanotubes while A_9K self-assembled into short nanorods (Figure 4).[19,20a]

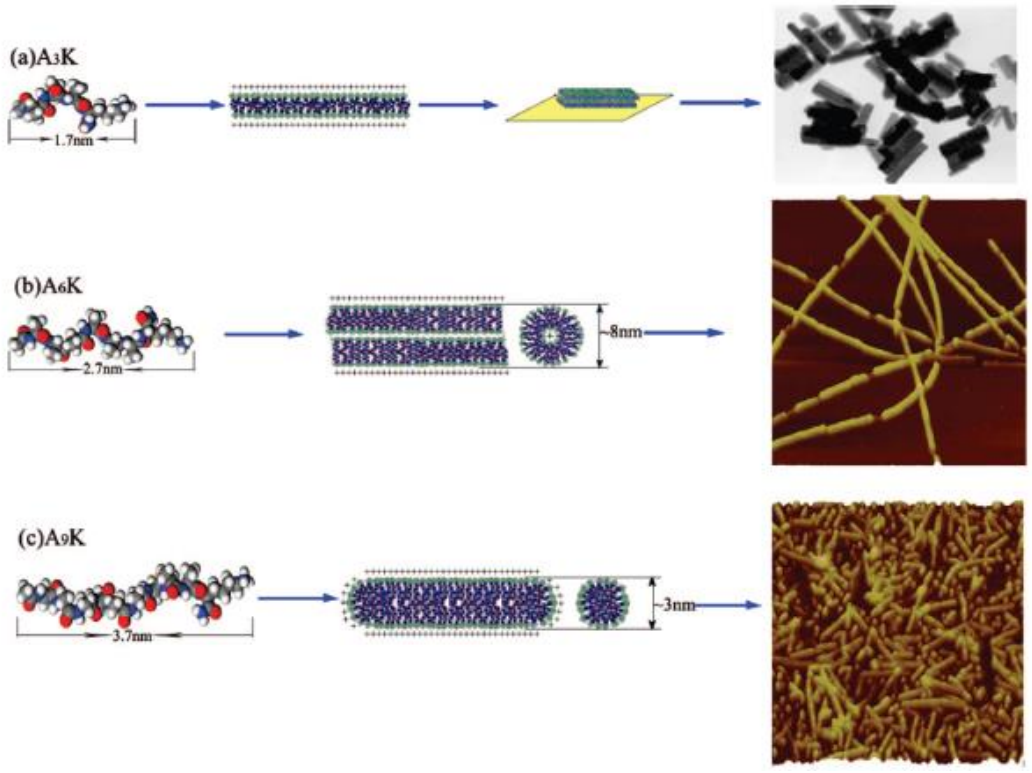

Figure 4. Schematic illustration of peptide surfactant self-assembly. (a) A_3K had the shortest chain and had no apparent critical aggregation concentration (CAC) detected, giving rise to the lowest effective a_e (equilibrium area occupied by each surfactant at the curved interface in the aggregate)

and the highest packing parameter; consequently, stacked A_3K bilayers were formed. (b) With increasing hydrophobic tail length and decreasing CAC of A_6K, the electrostatic repulsion between the head groups increased. This, together with the packing and entropic effect, led to the lowering of the packing parameter and the formation of nanofibers. (c) A_9K had the lowest CAC, the highest electrostatic repulsion between head groups, and the largest entropic effect arising from the longest tail, resulting in the lowest *p* and the formation of nanorods. In each case, lysine (K) groups remained at the outer surface of the nanostructures formed. Reprinted with permission from ref. 19. Copyright 2013 American Chemical Society.

The nanofibers formed by A_6K had the uniform diameter of 8 nm with quite flexible in nature. Transmission Electron Microscopy (TEM) image of A_9K showed the formation of thin and short nanorods with a diameter of 3 nm and length of 100 nm. The trend is consistent with packing theory extensively used for common surfactants.

A dialkyl tail containing PA was developed by Matthew et al.[20b] to design micelles as antigen delivery vehicles in *vivo*. Two palmityl chains (C_{16}) was conjugated to a peptide containing a cytotoxic T-cell epitope derived from ovalbumin. The peptide sequence was termed as OVA (EQLESIINFEKLTWE). DiC_{16}-OVA amphiphiles self-assembled into cylindrical micelles.

2.2. Nanofibers

Nanofibers are defined as fibers with a diameter size of less than 100 nanometer. Basically, the difference between nanofibers and nanotubes is that nanotubes are hollow structures. Herein,

we discuss the nanofibers formed by PAs and peptides with alternating hydrophobic and hydrophilic amino acids

2.2.1. PAs as Nanofibers

This category of structures is mostly generated by PAs, which consist of hydrophobic alkyl tails and hydrophobic heads, similar to lipids. Phospholipid membrane in the biological systems also composes of a hydrophilic head and a hydrophobic tail. PAs self-assemble into ordered structures in water through hydrophobic interactions. PAs have the structural features of both amphiphilic surfactants and functions of bioactive peptides. These molecules generally assemble in water into nanofibers at specific solution conditions (temperature, pH, and ionic strength). Furthermore, it has been demonstrated that stable nanofibers can be formed by mixing two oppositely charged PA molecules to support favorable ionic interactions.[21]

A broad class of amphiphilic molecules has been used to create organized biomaterials by Stupp and co-workers. For example, an artificial 3D scaffold consisting of nanofiber networks was formed by the aggregation of the amphiphilic molecule IKVAV. This process was triggered by the addition of neural progenitor cell suspensions to the aqueous solution.[22] The investigators used the 3D network of nanofiber scaffold to encapsulate cells in vitro which promoted very rapid differentiation of cells into neurons.

To investigate the nature of the interiors of self-assembled cylindrical aggregates, Stupp and coworkers explored fluorescence techniques using fluorophores, such as tryptophan or pyrene, in the peptide backbone.[23] PAs bearing fluorophores (tryptophan or pyrene) when self-assembled at low pH and exhibited differing degrees of exposure to the solvent and accessibility to the

quencher. Interior of tryptophan bearing amphiphiles nanostructures remained well solvated irrespective of the positions of fluorophore, suggesting easy access of hydrophilic molecules inside the aggregates. Stern-Volmer quenching analysis, a method for quantifying the degree of solvent exposure of a protein, indicated different degrees of quencher (pyrene) infiltration into the nanostructures.

Stupp and his group also designed a series of PAs to make one dimensional cylindrical nanostructures. PAs containing hydrophobic alkyl chains self-assemble into nanofiber structures because of hydrophobic collapse and β-sheet formation.[24] Upon pH changes, these PAs formed aqueous gels. The stability of these materials can be increased by reversible polymerization. Their one dimensional fiber structures were restricted when theses PAs were mixed with dumbbell-shaped template containing hydrophobic oligo (*p*-phenylene ethynylene) core.[25] Atomic Force Microscope (AFM) and TEM data revealed a significant change in the PA supramolecular aggregation from nanofibers to small monodisperse nanostructures upon the addition of the dumbbell shape scaffold.[25]

Self-assembly of PAs into nanofibers was also triggered by light as shown by Stupp and his group.[27a] A photoacid generator (PAG) was introduced to lower the pH upon exposure to light to promote the self-assembly of the pH-responsive PAs inside liposomes. Encapsulation of PAs within the aqueous interior of liposomes was carried out by using a PA solution to hydrate a phospholipid film. The light-triggered PA self-assembly and encapsulation were confirmed by confocal fluorescent microscopy, Scanning Electron Microscopy (SEM), Fourier Transform Infrared Spectroscopy (FTIR), and circular dichroism (CD). The investigators proposed that packed nanofibers within the interior of liposomes could have potential application in targeting specific tissues or tumors.

Self-assembly of amphiphilic oligopeptide consisting of arginine headgroups into fibril structures was investigated by Hamley et al.[27b] Alanine-rich peptide $A_{12}R_2$ containing twelve alanine residues and two arginine residues was synthesized via *N*-carboxyanhydride (NCA)-polymerization method. Self-assembly was driven by the electrostatic repulsion between the arginine headgroups, leading to the formation of twisted fibril and stacking of alanine residues.

Castelletto *et al* explored the possibility of self-assembly of a bioactive dipeptide L-Carnosine (βAH, where A = alanine, H = histidine) by incorporating a bulky aromatic substituent.[27c] Fmoc [(*N*-(fluorenyl-9-methoxycarbonyl)], commonly used as protecting agent in solid-phase peptide synthesis has been used as structure-directing agent to induce fibrillization of carnosine. Fibrillization of carnosine occurred via π-π stacking interaction. They also demonstrated that this Fmoc-peptide retained the chelating property with Zn^{2+} ions even after fibrillization. They further extended their work by incorporating a lipid chain with L-carnosine to investigate the self-assembly of βAH.

C_{16} palmitoyl lipid chain has been used as structure-directing agent to induce the fibrillization of βAH.[27d] PA hexadecyl-(β-alanine-histidine) (C_{16}-βAH) self-assembled into nanotape structures due to the hydrophobicity and excluded volume constraints imposed by the lipid tail. The investigators further demonstrated that the addition of C_{16}-βAH to DPPC (dipalmitoyl phosphatidylcholine) multilamellar vesicles led to the formation of well-defined unilamellar vesicles.

The self-assembly behavior of commercially available PA, matrixyl consists of palmitoyl (C_{16}) hydrophobic chain and peptide KTTKS was investigated by Valeria et al.[27e] C_{16}-KTTKS was incorporated into antiwrinkle skin care creams with the trade name of Matrixyl. This compound

self-assembled in a relatively dilute solution. The acetate salt of this PA formed a giant fibrillar structures with several micrometer length. Investigation at the nanoscale revealed extended tape structures with a persistent length extending to ten of microns or more. Small angle X-ray scattering (SAXS) indicated a bilayer structures within the tape. In contrast, the TFA salt of peptide amphiphile C_{16}-KTTKS exhibited temperature-dependent self-assembly behaviour. [27f] At higher temperature, it formed micelles instead of nanotape structures. At low temperature, β-sheet nanotape was stabilized by hydrogen bonding whereas hydrogen bonding was disrupted at higher temperature. Self-assembly of C_{16}-KTTKS was fine-tuned by adjusting the pH of the solution.[27g] As the pH decreased from 7 to 4, a transition in morphology occurred from tape to twisted fibrils. Again it formed tape like structures at lower pH (pH 3). In contrast, spherical micelles were observed at pH 2. Nanotape structures were also found when C_{16}-KTTKS was mixed with C_{16}-ETTES.[27h] Electrostatic interactions between anionic residue E (glutamic acid) and cationic residue K (lysine) led to the formation of fibrillar self-assembled structures.

Self-assembly of tryptophan containing PA C16-W3K exhibited transition in morphology from spherical micelles to worm like micelles.[27i] Initially, it showed discrete spherical micelles structures of diameter about 10 nm. In contrast, after 13 days it exhibited long nanofibrillar structures with outer diameter of approximately 10 nm. It was hypothesized that the transition was probably due to the peptide configurational transition. The CD results indicated that the secondary structure of the molecule changed from mixture of α-helix and random coil to β-sheet with time without any external stimuli.

PAs also self-assembled into nanostructures in presence of macromolecules. The cationic Lys-PA self-assembled (C12-VVAGK-Am) into nanofiber in presence of *Bcl-2* antisense oligonucleotide (ODN) through electrostatic interaction.[27j] This conjugate was investigated for the

slow release of ODN from the nanofiber network. Moreover, it delivered the antisense oligonucleotide efficiently inside the cells in controlled way, which resulted the down regulation of *Bcl-2* mRNA levels, indicating the potential use of PA in gene targeted therapy.

Self-assembly of bacteria-derived lipopeptides was investigated by Hamley et al.[27k] The lipopeptides surfactin, plipastatin, and mycosubtilin consisting of cyclic peptide head groups and different alkyl chains were obtained from *Bacillus subtilis*. Surfactin and plipastatin self-assembled into spherical micelles whereas mycosubtilin formed extended nanotape structures. The distinct mode of self-assembly of mycosubtilin compared to the other two peptides was attributed due to the differences in the surfactant packing parameters.

Polymer containing PAs have been designed and the bioactivity of the self-assembled structures has been investigated by Valeria et al.[27l] Peptide DGRFFF containing the RGD cell adhesion motif was conjugated with poly(ethylene glycol) (PEG) chain of molar mass 3000 kg mol^{-1}. At high concentration the polymer-peptide conjugate formed nanofibril structures despite the presence of crystallization of PEG, which occurs during drying process, indicating the strong tendency of aggregation of the conjugate. Cell proliferation was observed in presence of the conjugate at optimum concentration.

Incorporation of titanium-based biomaterials in the existing tissues is one of the key problems in the area of orthopaedic and dental implants. To address this biocompatibility issue, Hakan et al demonstrated the biofunctionalization of titanium by immobilizing a bone ECM-mimetic self-assembled peptide nanofiber on the metal surface.[27m] To accomplish this, two PAs were designed. In one sequence, PA molecule (Lauryl-VVAGE) was covalently conjugated to Dopa (3,4-dihydroxy-L-phenylalanine) which showed strong binding with hydrophilic surface.

Another PA molecule (Lauryl-VVAG) was conjugated to a heparin binding adhesion peptide sequence, KRSR. These conjugated molecules Lauryl-VVAGE-Dopa-Am (Dopa-PA) and Lauryl-KRSR-Am (KRSR-PA) exhibited self-assembled nanofiber structures driven by electrostatic interaction at the physiological pH via β-sheet formation.

A PA molecule incorporating photocleavable groups between hydrophobic and peptide domains were designed by Muraoka et al.[28] This PA molecule consisted of a 2-nitrobenzyl group, a palmitoyl tail, and an oligopeptide segment $GV_3A_3E_3$. The 2-nitrobenzyl group was covalently linked to the *N*-terminal amide of the glycine residue and was cleaved by irradiation at 350 nm (Figure 5). This PA molecule containing the photocleavable group self-assembled into quadruple helical fibers, which was converted to a nonhelical fibril upon irradiation.

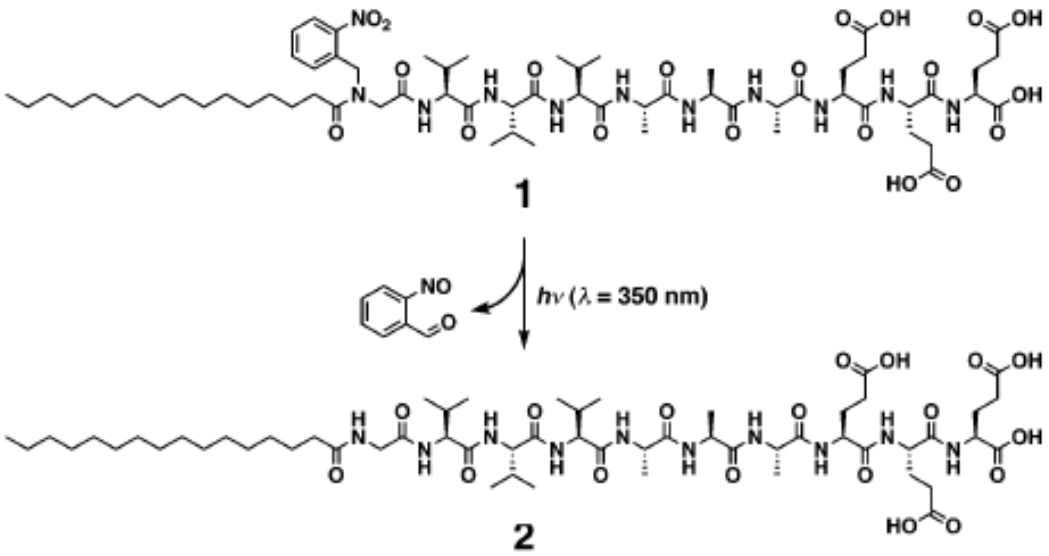

Figure 5. Cleavage of 3-nitrobenzyl group from a PA molecule consisting of a 2-nitrobenzyl group, a palmitoyl tail, and an oligopeptide segment $GV_3A_3E_3$. Reprinted with permission from ref. 28. Copyright 2013 American Chemical Society.

2.2.2. β-Sheet Peptides with Alternating Hydrophobic and Hydrophilic Amino Acids as Nanofibers

The β-sheet structure, along with the α-helix, is one of the major secondary structural elements in proteins. The polypeptide chains remain as extended β-sheet structure. The nearby β-strands can lie in either a parallel or an antiparallel fashion. In both fashions, the orientation of the β-strands become such a way that alternate amino acid side chains remain towards the opposite sides of the sheet. Sometimes, the electrostatic and hydrophobic forces among the amino acid side chains stabilize the sheets.

Peptides containing alternating hydrophilic and hydrophobic amino acid residues are known to have a strong tendency to generate β-sheet structures.[26,29] Alkylated peptide amphiphiles consisting of hydrophobic and negatively charged residues (V and E) and an alkyl chain with 16 carbons ($C_{16}H_{31}$OVEVE) self-assembled into flat 1D giant nanobelt structures.[26] The structural template of VEVE flips the hydrophilic and hydrophobic side chains to the opposite sides of the peptide amide backbone when adopting an extended β-strand conformation. It was hypothesized that hydrophobic valine residue had a tendency to form a dimer to avoid exposure to water. Tapping-mode AFM imaging revealed the flat, belt like morphology of the nanostructures formed in aqueous solution over the course of 2 weeks. The investigators assumed that the alternating sequence of amino acids led to more effective chain packing within the peptide region and formation of the nanobelt morphology (Figure 6).

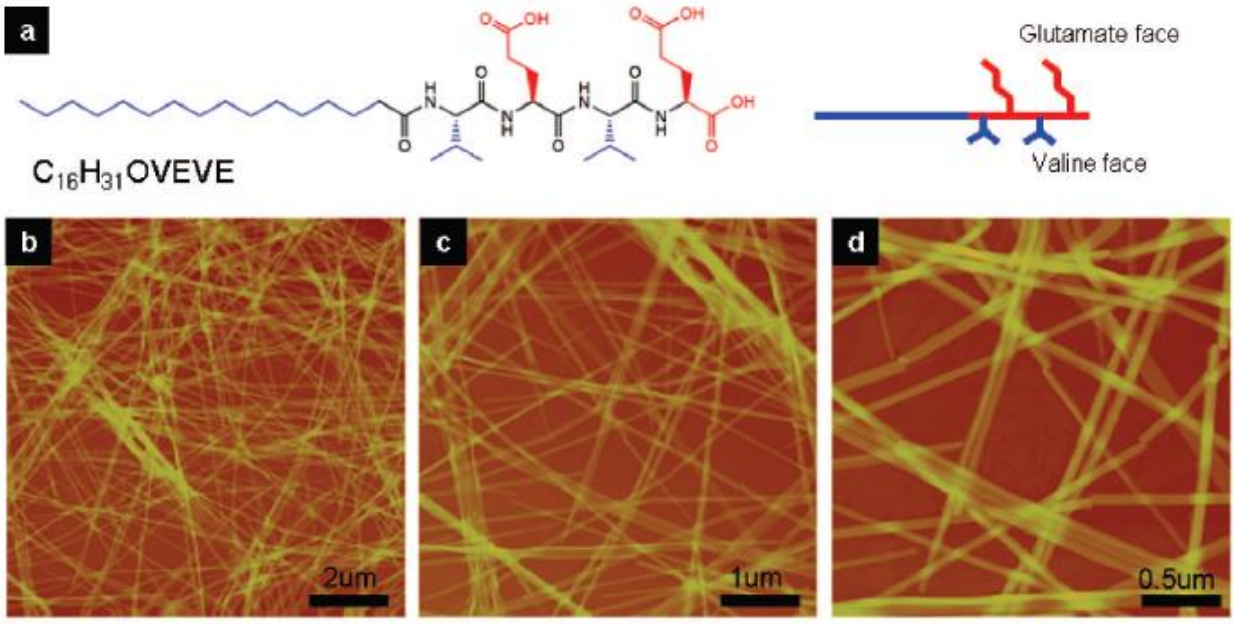

Figure 6. Nanobelts assembled from a PA containing four amino acids and an alkyl tail. (a) Chemical structure of the PA. (b-d) AFM images of peptide nanobelts at different scanning sizes. The assembled nanobelts are the dominant structures in the assembly system (almost artifact free). Reprinted with permission from ref. 26. Copyright 2013 American Chemical Society.

Interestingly, replacing the VEVE peptide segment with a structural motif of VVEE having different sequence of amino acids residues led to the formation of cylindrical nanofibers under similar conditions (Figure 7). On the other hand, when alternating sequence of VEVE was replaced with VVEE, the cylindrical curvature was regained back as shown in Figure 7.

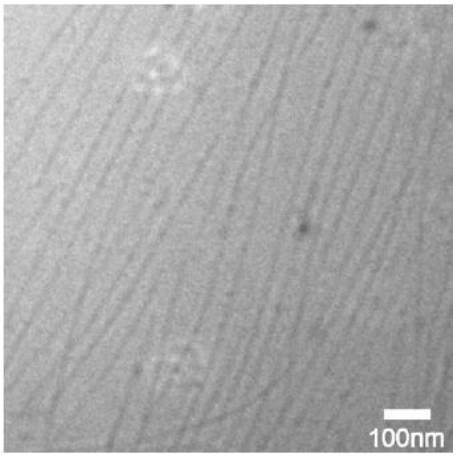

Figure 7. Cryo-TEM image of 0.1 wt % $C_{16}H_{31}$OVVEE aqueous solution clearly demonstrates cylindrical nanofibers. Reprinted with permission from ref. 26. Copyright 2013 American Chemical Society.

Short peptide KFE8 (FKFEFKFE) having an alternating pattern of hydrophobic and hydrophilic amino acids was shown to form self-assembled nanofiber structures. Mechanistic studies showed that it formed helical ribbon initially, which transformed into fibrillar structures.[30] Molecular dynamics simulation revealed the possibility of double helical β-sheet formation. Later, Matsuura et al. extended the work by designing three way junctions, C_3-symmetric conjugate trigonal $(FKFEFKFE)_2$ consisting of three β-sheet-forming peptide FKFEFKFE (Figure 8).[31] This peptide conjugate self-assembled into viral-sized peptide nanospheres. The above mentioned conjugate was soluble in acidic water but was hardly soluble in neutral and alkaline water. The CD spectrum of this peptide in aqueous HCl showed negative peak at 219 nm, suggesting the formation of β-sheet structures. Another negative peak at 200 nm was probably attributed to an induced CD for the benzene ring or amide bonds of the core molecule, since a CD peak was not observed for the component peptide FKFEFKFE alone. On the contrast, FT-IR showed bands

which were characteristic of antiparallel β-sheet structures. These combined results clearly indicate that this trigonal peptide forms hydrogen-bond-mediated intermolecular assemblies as it is not possible for a single trigonal $(FKFE)_2$ molecule to form β-sheets in an antiparallel manner. The investigators proposed that this strategy could be widely applied to the design of spherical bio-nanoassemblies.

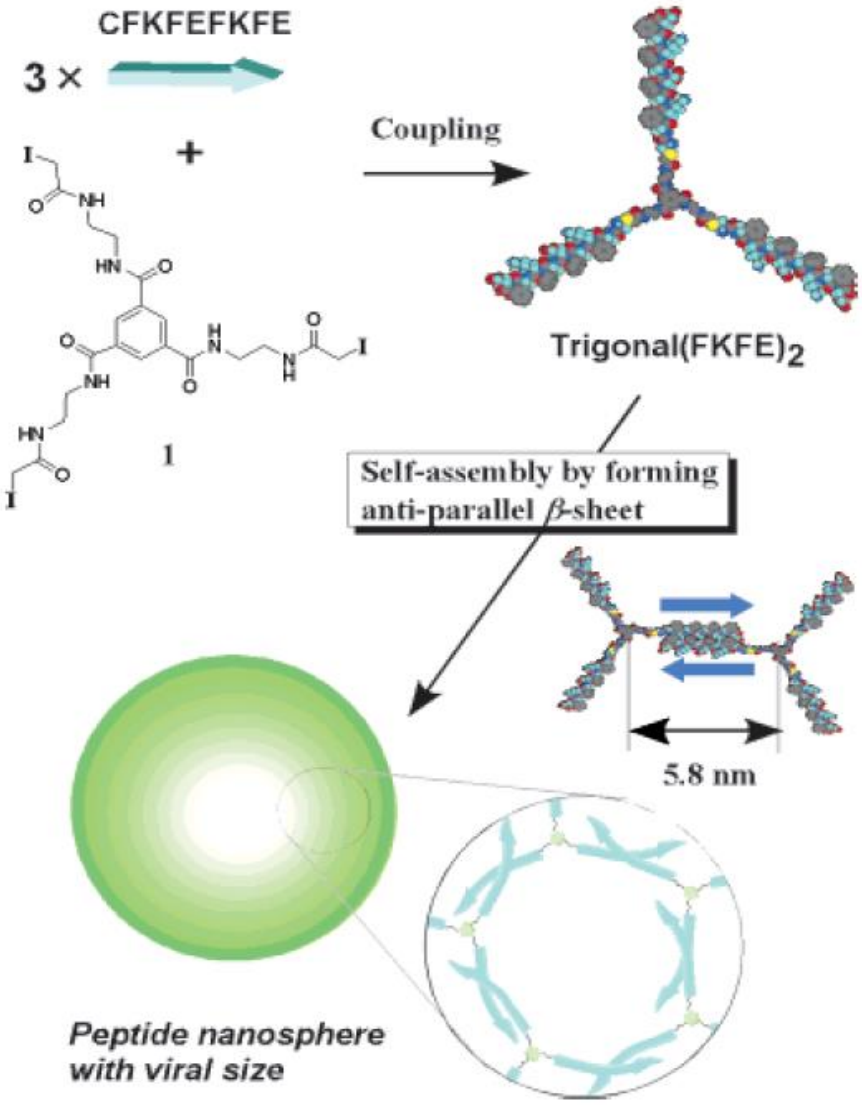

Figure 8. Synthesis of a *C*3-symmetric β-sheet peptide conjugate and schematic illustration of the self-assembly. Reprinted with permission from ref. 31. Copyright 2013 American Chemical Society.

Stimulus-responsive peptide self-assembly provides a powerful approach to control the self-assembly as a function of environment. Various stimuli-responsive systems including pH, ionic strength, temperature, light, and enzymes have been designed for peptide self-assembly. Recently, additional microenvironment-sensitive triggers for self-assembly was developed by Bowerman et al.[32a] The investigators explored the concept of reductive trigger for peptide self-assembly. The amphipathic Ac-$(FKFE)_2$-NH_2 sequence, known to form self-assembled fibril nanostructures, when flanked with a cysteine (Cys) residue, Ac-C$(FKFE)_2$CG-NH_2, it formed macrocyclic structure via disulfide bonding and prevented the β-sheet formation that was needed for self-assembly. On reduction of this disulfide bond, the peptide transformed into the stable β-sheet conformation which resulted into self-assembled fibrillar structures. At sufficient peptide concentration, it formed rigid hydrogels with viscoelastic properties (Figure 9).

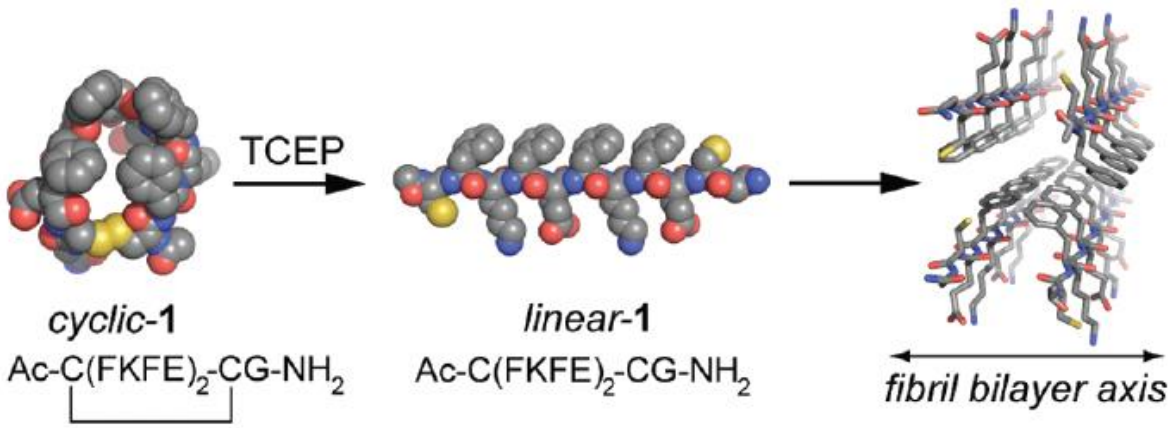

Figure 9. Cyclic to linear peptide conformational switch using a reductive trigger. Reprinted with permission from ref. 32a. Copyright 2013 American Chemical Society.

2.3. Other Peptides with β-Sheet Structures

Traditionally, peptides are made chemically or using genetic engineering for studying the self-assembly process. These methods are expensive and time consuming. Moreover, it is really challenging to design the proper sequence to achieve the desired morphology. Jinming et al., demonstrated one simple method to obtain an octapeptide sequence, GAGAGAGY, from the natural resource, *Bombyx mori* silk fibroin.[32b] Based on this sequence, a PA, C_{12}-GAGAGAGY was constructed and its self-assembly nature was investigated. It formed cylindrical nanofibers at pH 9 and twisted nanofibers at pH 4, indicating the involvement of electrostatic interactions in the self-assembly process.

The incorporation of self-organizing peptides into synthetic polymeric materials has been investigated by various research groups. This kind of peptide-polymer bioconjugate is well documented in the literature.[32c,32d] It was found that alanylglycine (AG) repeating units formed extended β-strands in a variety of AG-rich polypeptides. On the basis of this idea, polypeptides containing repetitive sequence $[(AG)_xEG]_n$ (x = 3-6) was made, which formed extended-plate-like assembled structures. When $[(AG)_3EG]_n$ β-sheet polypeptides were conjugated to polyethylene glycol (PEG) end blocks, it prevented the macroscopic aggregation of the β-sheet blocks into needle-shaped lamellar crystals.[33a] However, it led to the formation of well-defined fibrils. Microscopy data suggested that fibril formation occurred in the β-sheet stacking direction which resulted in an assembly in which the hydrophobic β-sheet surfaces were screened from the polar solvent, whereas the PEG chains were in contact with the environment.

The hydrophobic-hydrophilic balance plays a key role in peptide self-assembly/disassembly process. To address this issue, Joris et al. demonstrated the disassembly of the peptide sequence Ac-KTVIIE-NH_2 by manipulating hydrophobic-hydrophilic balance.[33b] To investigate the effect of hydrophilic group in the self-assembly process, a PEG group was introduced on the *C*-terminus of the fibril forming peptide. The resulted PEG-peptide conjugate did not exhibit any assembled structure, presumably due to the high hydrophilicity. However, upon introducing the hydrophobic tail *via* photocleavable linker on the *N*-terminus fibril structure returned via β-sheet formation. When the hydrophobic tail cleaved on UV radiation, β-sheet structure was disrupted and consequently the fibrillar structure was damaged.

Peptides adopting β-sheet secondary structures have been suggested to be useful for various applications, such as nanowires, fibers for biomedical purposes, scaffolds in tissue engineering, or to direct transport.[34] However, only short fibers up to 4 μm in length are accessible. To achieve extended and strong nanofibers, which is stable enough to mechanical stress and eventually more useful in materials science, peptides with a higher tendency to form stable aggregates, are needed. However, the solid-phase supported synthesis (SPPS), purification, and analysis of these peptides is actually difficult. To address this issue, Hentschel et al studied peptide guided assembly of polyethylene oxide (PEO)-peptide conjugate (Figure 10).[35] The peptide containing valine and threonine, [$(Thr\text{-}Val)_5$], which has a high β-sheet propensity and aggregation tendency, was conjugated to PEO and an acid labile linker was used to liberate PEO-peptide conjugate from the solid support. This conjugate organized into a long, nonbranched fibers of width about 2 μm and lengths up to several millimeters.

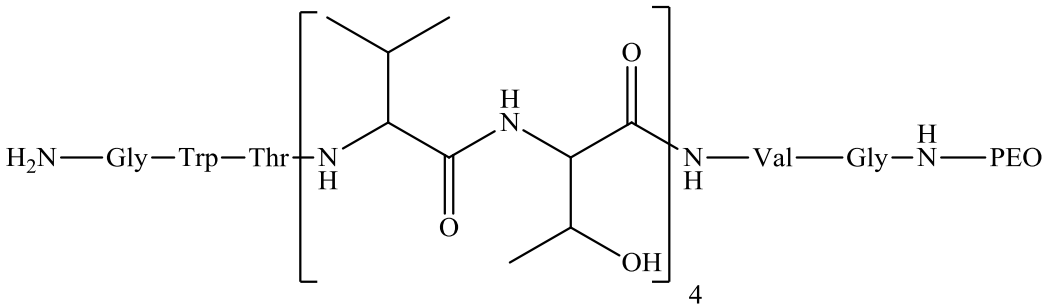

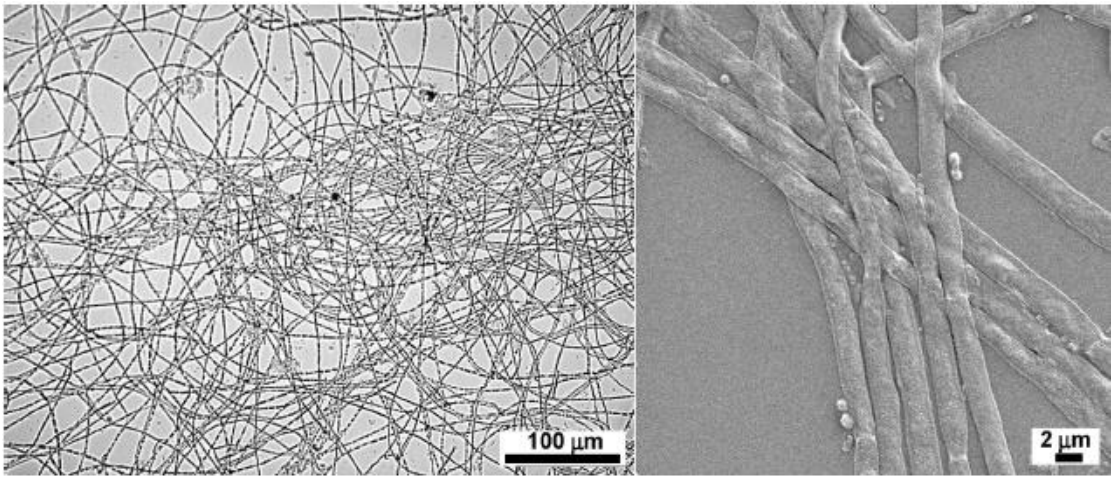

Figure 10. Spontaneously formed aggregates by peptide guided assembly of PEO-peptide conjugate. Light microscopy (left) and SEM micrograph (right). Reprinted with permission from ref. 35. Copyright 2013 American Chemical Society.

Most of the artificial β-sheet peptides are designed in such a way that the polar and hydrophobic amino acids are placed alternatively. This kind of arrangement promotes the

hydrogen bonding between amide hydrogen and carbonyl oxygen. When one side of the β-sheet contains hydrophobic amino acid residues, removal of hydrophobic residues from aqueous contact forces two β-tapes to associate into bilayered β-sheet nanoribbon (β-ribbon) structure. Recently, it was observed that coupling of a hydrophilic and bioactive peptide to a β-sheet forming peptide would enable the formation of 1D nanostructure decorated with bioactive peptides. Based on this idea, a supramolecular building block, Tβp was made which consisted of a cell penetrating peptide (CPP) Tat and a β-sheet forming peptide.[36,37]

It was found that the block peptide formed a β-ribbon structure in which β-sheet interaction was the main driving force for the self-assembly. The Tβp β-ribbons (Figure 11) were able to encapsulate hydrophobic guest molecules, such as pyrene or Nile red, in the hydrophobic space between two β-tapes. Moreover, it was observed that cell penetration efficiency of the Tβp β-ribbon was much higher than that of Tat-CPP only, suggesting that the multivalent coating of CPPs is advantageous in increasing cellular uptake efficiency.

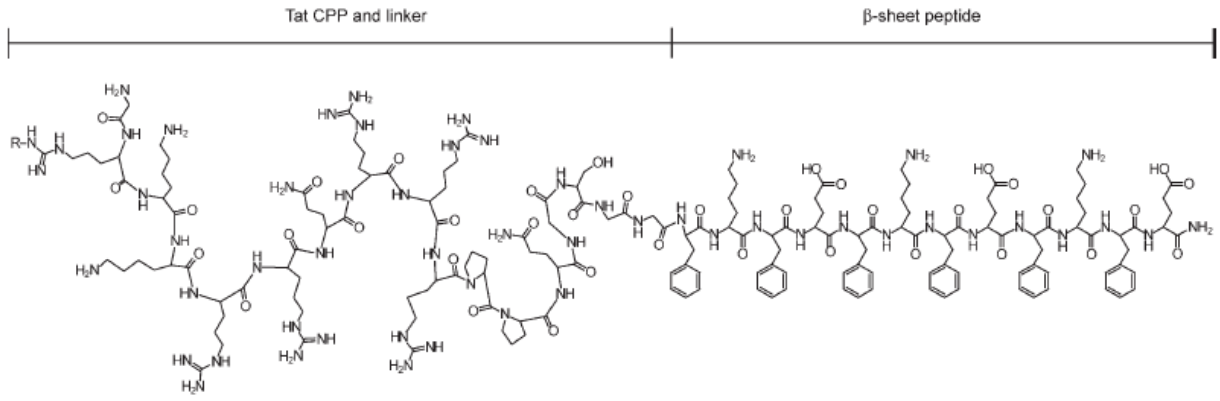

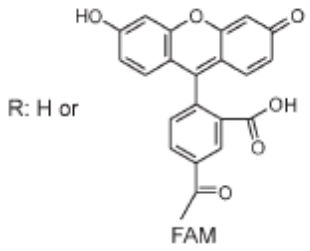

Figure 11. Structure and sequence of TβP peptides. Reprinted with permission from ref. 36. Copyright 2013 Wiley Publishing Group.

2.4. Vesicle/Spherical Structures

Amphiphilic oligopeptides consisting of various ratio of hydrophilic to hydrophobic block length are able to self-assemble into vesicular structures in aqueous solution at neutral pH. It has been shown by Van-Hell et al. that hydrophilic compounds could be encapsulated within the peptide vesicles.[18] These peptides were recombinantly produced in bacteria as an alternative to solid-phase synthesis. Other types of peptides that could be self-assembled to vesicles were copolypeptides, proline-rich peptides, and cyclic peptides.

2.4.1. Copolypeptides

Deming and coworkers reported the self-assembly behavior and application of poly(L-lysine)-b-poly (L-leucine), poly (L-glutamic acid)-b-poly (L-leucine), and poly(L-arginine)-b-poly (L-leucine) diblock polypeptides, where 'b' denotes block.[38-40] Charged amphiphilic block copolypeptides formed stable vesicles and micelles in aqueous solution. Aqueous self-assembly of opposite charged poly(L-lysine)-b-poly(L-leucine) and poly(glutamic acid)-b-poly(L-leucine)

block copolypeptides led to the formation of unilamellar vesicles.[38] The driving force for the aggregation of the diblock polypeptides was the α-helical hydrophobic rod formation of the poly(L-leucine) block. The diblock polypeptides formed vesicular structures at low hydrophobic residue contents (10-40 mol%). Amphiphilic diblock copolymers formed small spherical or cylindrical micelles in this composition range, and vesicle structures were found at higher hydrophobic contents (approximately 30–60 mol%). This divergence was attributed to the rigidity of the chain conformation and strong interactions. The polyarginine coated vesicles showed potential as intracellular delivery following entrapment of hydrophilic molecules. The guanidine groups of arginines as crucial residues of cell penetrating peptides were responsible for the effective delivery of the vesicles and cargos.

Holowka et al. used Texas Red labeled dextran, a water soluble cargo, to check the integrity of the vesicle membrane of poly(L-lysine)-b-poly(L-leucine). The cargo was encapsulated during vesicle assembly and after dialysis.[39] Formed vesicles showed to contain encapsulated dextran. Though positively charged polypeptides were relatively unstable, whereas negatively charged polypeptides vesicles were quite stable.

Rodriguez-Hernandez et al. reported pH sensitive vesicles formation for zwitterionic diblock copolypeptides containing poly-L-glutamic acid-b-poly-L-lysine (PGA-b-PLys).[41] Copolypeptides changed from a random coil conformation into a neutral and α-helical structure (rod) after neutralization of the polypeptide block (Figure 12). At acidic pH, the PGA block was neutralized, which produced the vesicle in the core while the PLys block formed the shell. In contrast, under basic conditions, the protonated PLys block was converted into neutral and insoluble free $–NH_2$ groups that formed the core of the aggregates. It was assumed that the vesicle formation was attributed to the systematic presence of the polypeptide in a rod like morphology in

the hydrophobic part of the membrane, making a low interfacial twist and as a result, a hollow structure was formed.

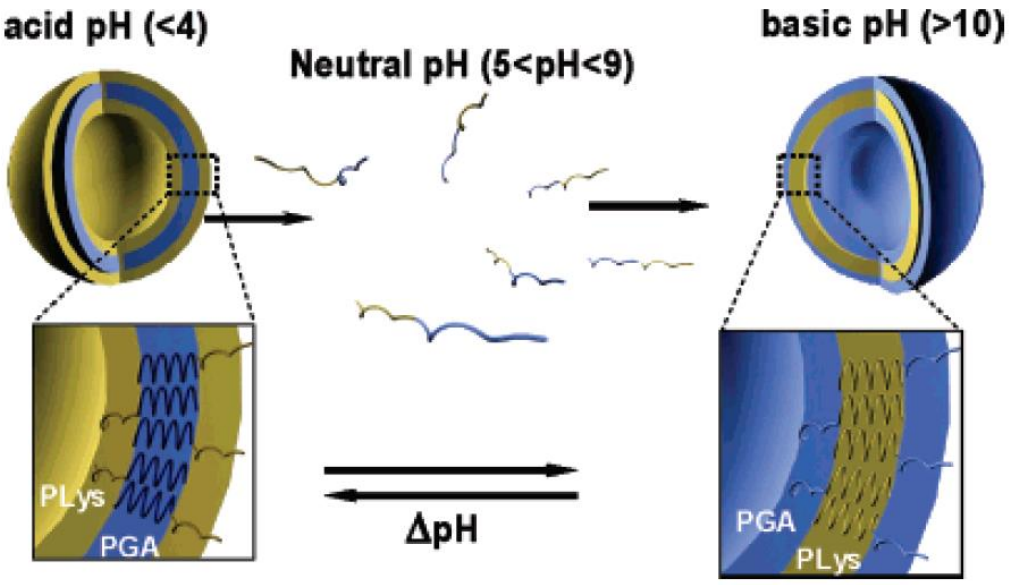

Figure 12. Schematic representation of the self-assembly into vesicles of the diblock copolymer PGA15-b-PLys15. Reprinted with permission from ref. 41. Copyright 2013 American Chemical Society.

Thermally sensitive polypeptides were developed by Dreher et al.[42] Temperature triggered self-assembly of elastin-like polypeptides (ELPs) in a linear AB diblock architecture into a spherical micelle was carried out through a small increase of temperature to between 37 and 42 °C. This temperature range is commonly used for clinical application of hyperthermia. The size of the micelle was controlled by both the length of the copolymer and hydrophilic-hydrophobic block ratio.

2.4.2. Proline-Rich Peptides

The self-assembly of proline-rich peptides was explored by Lee and his group.[43,44] Among naturally occurring amino acids, proline contains a pyrrolidine ring side chain and backbone atoms. In the cyclic structure of proline, conformational constraints are induced among the atoms in the pyrrolidine ring, which results the formation of stiff helical rod structures, polyproline type II (PPII) helix in aqueous solution. On the other hand, biologically active and hydrophilic peptide coil, Tat cell-penetrating peptide (CPP) is a highly charged peptide and forms a random coil conformation in aqueous solution. Arginine residues in Tat CPP play the key role in the cell binding and entry.

Lee and coworkers hypothesized that rigid rod character and the nonpolar nature of the outer surface of a PPII helix might impart microphase separation characteristics to the rod-coil of a PPII rod and a hydrophilic coil, leading to the anisotropic orientational ordering of the rod and self-assembly. Based on this idea, a block polypeptide of polyproline and an arginine oligomer, $P_{10}R_3$ was designed, and the self-assembly actions were investigated. The secondary structure of $P_{10}R_3$, consisting of 10 proline and 3 arginine residues showed characteristics of PPII helix. Microscopy data suggested the formation of vesicles rather than micelles (Figure 13). Another polypeptide P_{10}Tat also self-assembled into vesicular structures. Both peptides $P_{10}R_3$ and P_{10}Tat were introduced as potential carriers for delivering hydrophilic drug molecules into cells.

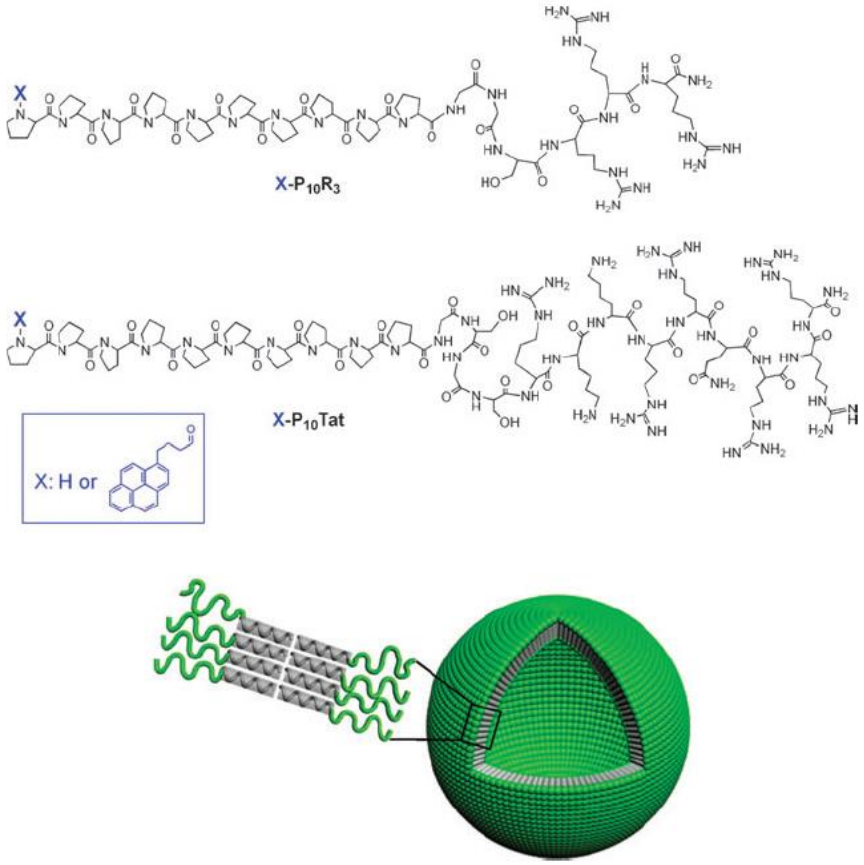

Figure 13. Structures of peptide rod–coil building blocks and their self-assembly into nanocapsule structures. Reprinted with permission from ref. 43. Copyright 2013 RSC Publishing Group.

2.4.3. Cyclic Peptides

Linear and cyclic peptides containing same sequence of amino acid residues showed differential behavior in the self-assembly process. Choi et al. reported that linear peptide containing tryptophan and arginine residues showed irregular morphologies whereas cyclic counterpart showed spherical nanostructures.[44] Recently, we have performed an extensive

investigation on the self-assembly process of a number of cyclic peptides including $[FR]_4$, $[FK]_4$, $[WK]_5$, $[CR]_4$, $[AK]_4$, and $[WR]_4$ containing L-amino acids (Figure 14).[45]

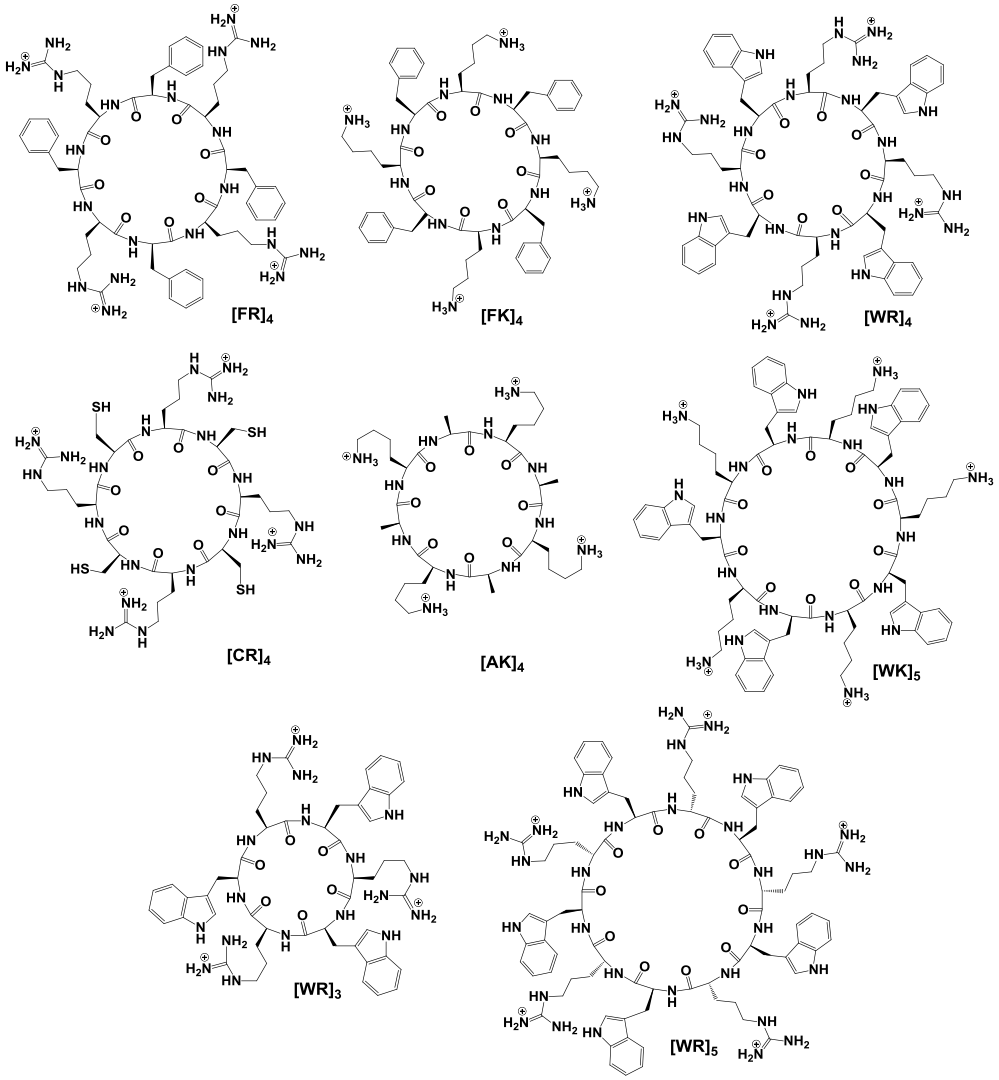

Figure 14. Chemical structures of synthesized cyclic peptides (F = phenylalanine, R = arginine, K = lysine, W = tryptophan, C = cysteine, A = alanine). Reprinted with permission from ref. 45.

The rationale behind the selection of amino acids in the structure of the peptide was based on the presence of alternating hydrophobic and positively charged residues or alternating neutral and positively charged residues in their structures. We hypothesized that the self-assembled nanostructures in aqueous solution could be formed through intramolecular and/or intermolecular interactions through an optimal balance of hydrophobicity and charge. Among all the designed peptides, one of the peptides, namely $[WR]_4$, generated self-assembled nanostructures at room temperature after a specific incubation time. The presence of the tryptophan's indole ring of in $[WR]_4$ was found to play a critical role in self-assembly process due to its high hydrophobicity through generating potential hydrophobic interactions. Furthermore, the presence of the positively charged guanidine group in the arginine was found to be involved in hydrogen bonding interactions. However, other 5 cyclic peptides did not show self-assembled nanostructures possibly due to inappropriate combination of hydrophobic and positively charged residues. As a result of the unique behavior of $[WR]_4$, and to investigate the role of the ring size, other derivatives in this group $[WR]_3$ and $[WR]_5$, were designed and tested to determine the effect of the ring size on the self-assembly process. TEM was used to investigate the morphologies of $[WR]_3$ and $[WR]_5$. All compounds in this class showed vesicle-type structures. TEM of $[WR]_3$ showed that this peptide forms structure within sizes of 100 nm after 14 days of incubation. $[WR]_4$ and $[WR]_5$ were observed in larger structures (550 and 930 nm, respectively) (Figure 15). The results indicated that three major elements are involved in the self-assembly process of these cyclic peptides including hydrophobic force, hydrogen bonding by partial β-structures, and/or the π- π stacking interactions between tryptophan residues.[45]

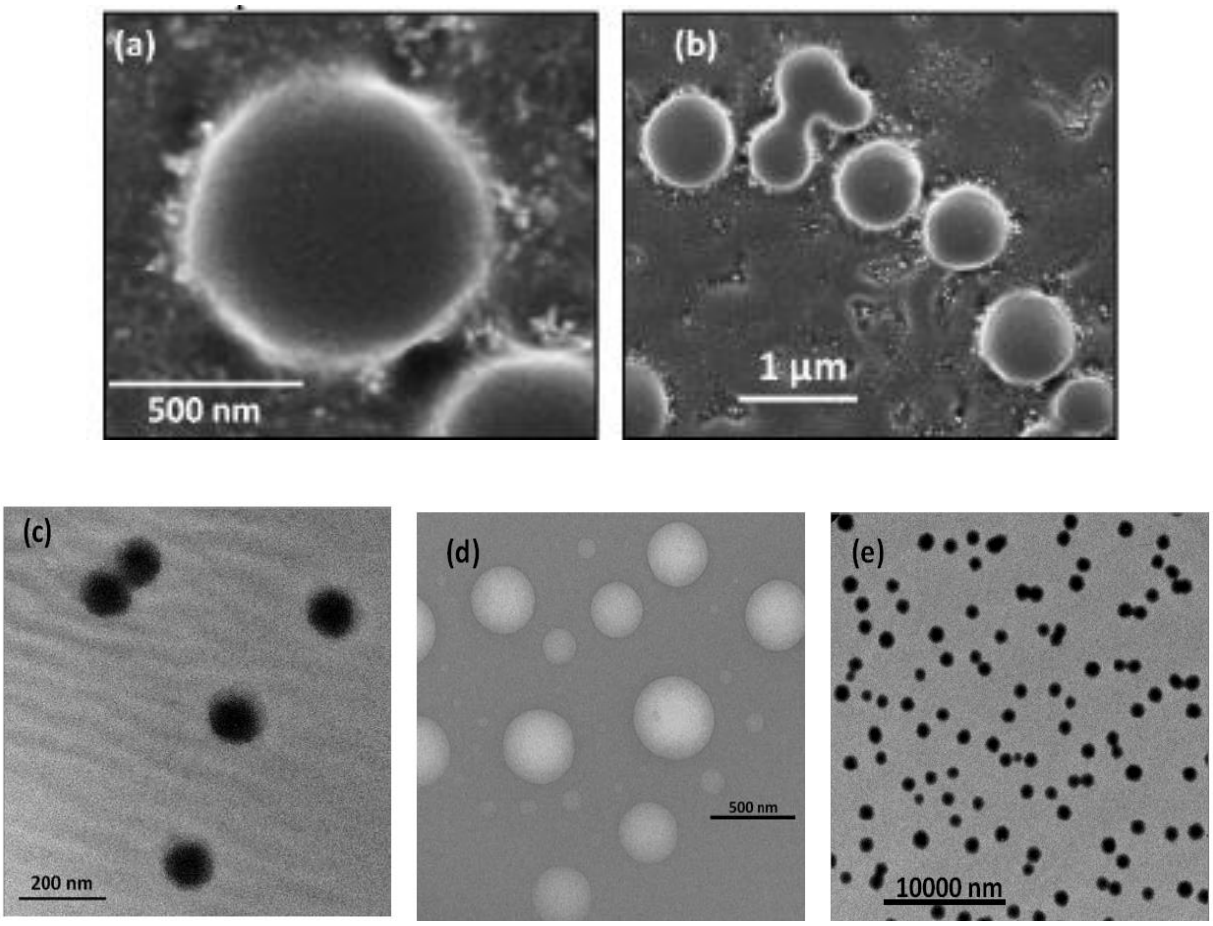

Figure 15. (a) and (b) FE-SEM image of self-assembled structure of $[WR]_5$ (2 mM) in water after 20 days; (c) TEM images of self-assembled structures of $[WR]_3$ in water after 2 weeks (without negative staining); (d) TEM images of self-assembled structures of $[WR]_4$ in water after 2 weeks (without negative staining); (e) TEM images of self-assembled structures of $[WR]_5$ in water after 2 weeks (without negative staining). Reprinted with permission from ref. 45.

We further investigated the new applications of this class of cyclic peptides for generating cyclic peptide capped gold nanoparticles (CP-AuNPs) as potential drug delivery purposes.[46] We

found out that the combination of tryptophan and positively charged amino acids worked as reducing/capping agents and led to the formation of *in-situ* functionalized metal nanoparticles.

Moreover, we noticed that the cyclic peptides containing alternative tryptophan and lysine (c[WK]$_5$) produce different gold nanoparticles when compared with their linear counterpart (l(WK)$_5$).[47] TEM investigations showed that l(KW)$_5$-AuNPs formed ball-shaped structures with the diameter size of 900−1000 nm (Figure 16). A large number of l(KW)$_5$-AuNPs were found to be in spherical morphologies and in the size range of 4−35 nm. The distribution pattern of AuNPs in of l(KW)$_5$-AuNPs was found to be an organized arrangement.

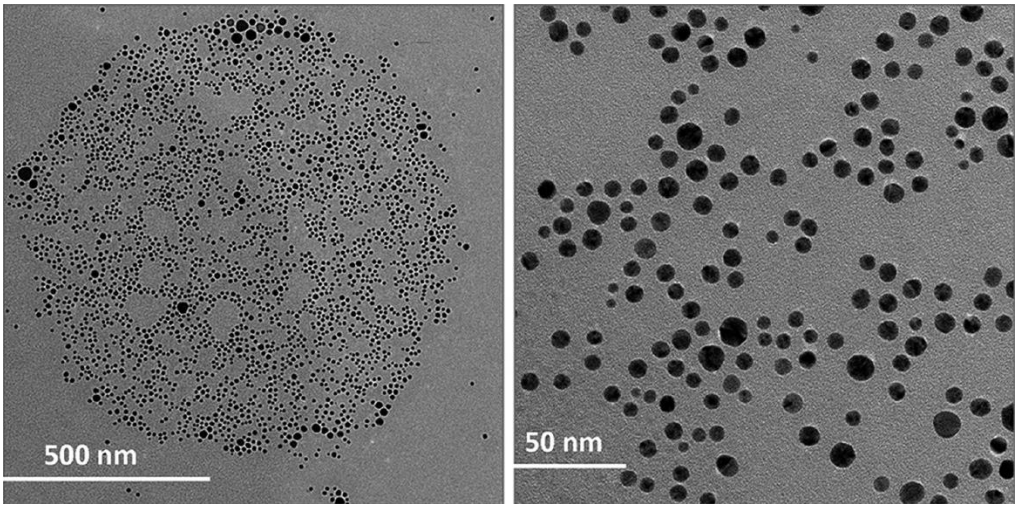

Figure 16. TEM images of l(KW)$_5$-AuNPs. Reprinted with permission from ref. 47. Copyright 2013 American Chemical Society.

Compared to linear peptide-capped AuNPs, TEM images of c[KW]$_5$-AuNPs showed sponge-like agglomerates. The spongy agglomerates were composed of peptide and AuNPs with

an approximate diameter size of 250−450 nm (Figure 17) along with some isolated AuNPs in spherical and triangular shapes (6−60 nm).

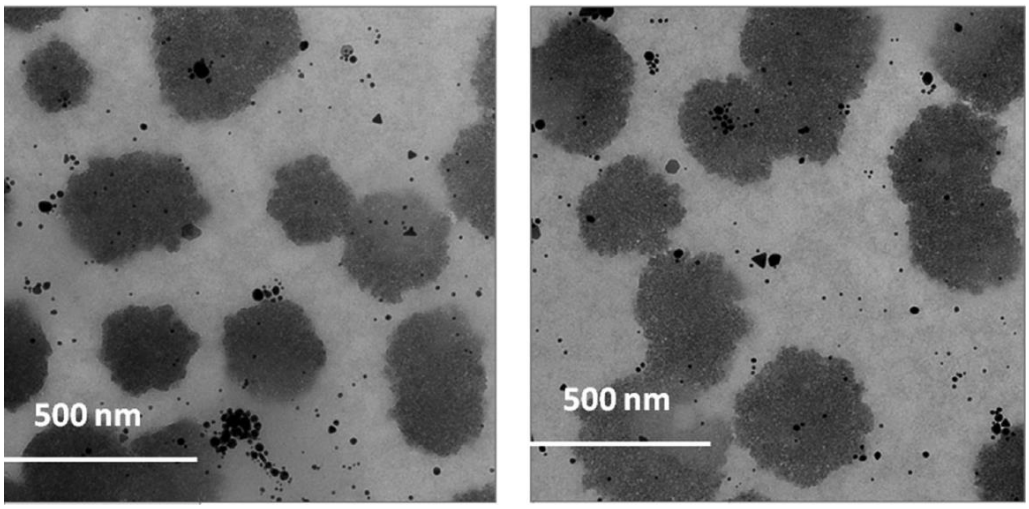

Figure 17. TEM images of c[KW]$_5$-AuNPs. Reprinted with permission from ref. 47. Copyright 2013 American Chemical Society.

These data suggested that the constrained nature of the peptide in c[KW]$_5$-AuNPs caused different orientation of amino acids in the secondary structure of peptide causing the formation of different environment surrounding the complex that led to the formation of organized morphologies by the peptides. This orientation altered the number of available amino acids such as tryptophan and/or lysine residues in reduction process of the Au^{3+}. However, l(KW)$_5$ more flexibility in the conformation compared to the corresponding constrained cyclic counterpart c[KW]$_5$ during the AuNPs formation. Additional positively charged amino groups and negatively charge carboxylates at *N*-terminal lysine and *C*-terminal tryptophan, respectively, could also participate in self-assembly process through intermolecular interactions of the peptide. Thus, the

cyclic and linear nature of the peptide and the orientation of amino acids were found to be the main reason for the different morphology and size of formed P-AuNPs.

Furthermore, the assemblies between a cyclic peptide ($[WR]_4$) as a drug delivery system and molecular cargos were investigated.[48] A negatively charged phosphopeptides (PEpYLGLD) was selected as a model cargo molecule. TEM investigation of negatively stained $[WR]_4$ alone showed circular vesicle-like structures with approximate size of 25−60 nm. TEM images of PEpYLGLD (Figure 18) exhibited mostly amorphous structures with approximate size of 40 nm. However, when PEpYLGLD was mixed with $[WR]_4$ in solution, PEpYLGLD-loaded $[WR]_4$ formed some larger noncircular morphologies with width and height of 125 and 60 nm, respectively.

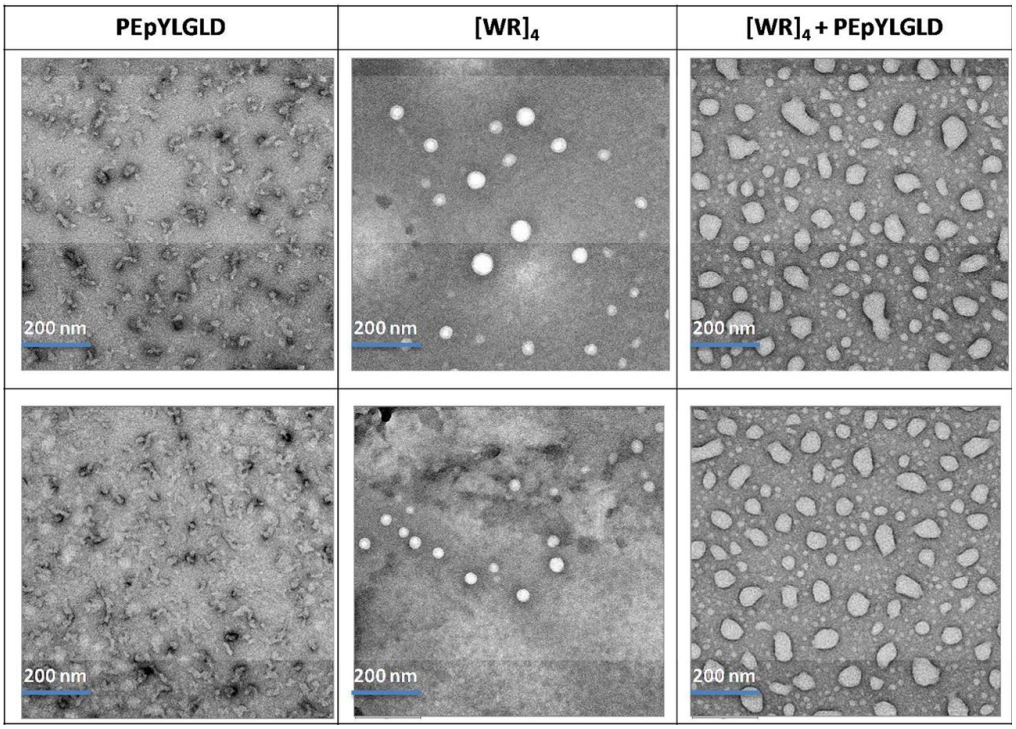

Figure 18. Negatively stained TEM images of $[WR]_4$ (1 mM), PEpYLGLD (1 mM), and PEpYLGLD-loaded $[WR]_4$ (1 mM) in water after one day. Reprinted with permission from ref. 48. Copyright 2013 American Chemical Society.

We proposed that the available electrostatic and/or hydrophobic intermolecular interactions between the positively charged cyclic peptide and negatively charged phosphopeptides was responsible for the self-assembly process (Figure 19). The structure of $[WR]_4$ was investigated by using TEM microscopy showing modified morphologies upon binding with PEpYLGLD by generating new nanostructures.

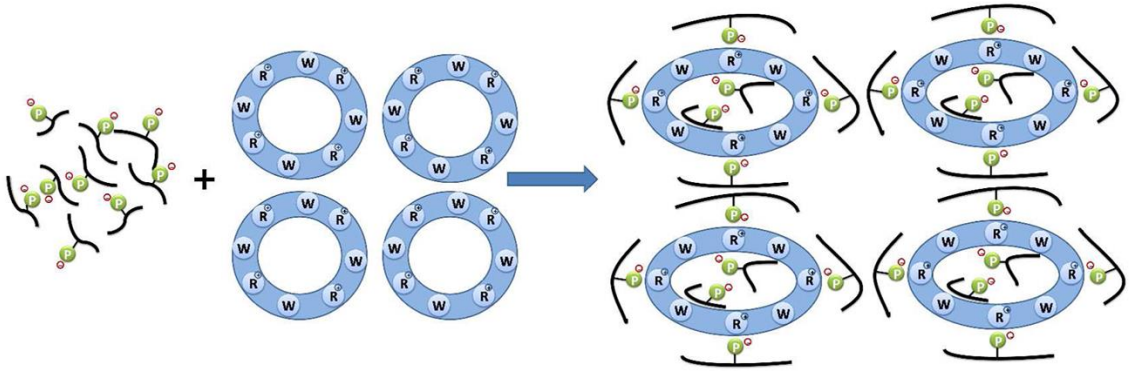

Figure 19. Proposed mechanism of the self-assembly and interactions between PEpYLGLD and $[WR]_4$. Reprinted with permission from ref. 48. Copyright 2013 American Chemical Society.

In conclusion, our efforts were focused on developing new sequences of amino acids in the structure of cyclic peptide for biomedical applications.[49,50] Our findings showed that the cyclic nature of the peptide was a critical element in the self-assembly process and their biological

activity possibly because of the constrained structure and different orientation of amino acids in their secondary structure.

2.5. Amyloid Nanofibrils

The self-assembly of peptides and proteins into fibrillar structure formation is very common phenomena in biological systems. Amyloid fibrils are key examples of protein self-assembly into nano-fibrillar structures.[51] The accumulation of amyloid fibrils is a common characteristic of various diseases including Alzheimer's disease, type II diabetes, Parkinson's diseases, and many others.[52] Furthermore, self-assembled nanofibrils generated from natural or artificial peptides have been suggested for potential application in bionanotechnology. Amyloid fibrils have β-sheet conformation generated by polypeptides of 30-40 amino acids or longer. It has been shown that short peptide fragments, for example, tetra- to hexapeptides, form fibrillar structure with similar biophysical and structural properties of amyloid fibrils.[53] Thus, they can be used as a model system for studying amyloid fibrils formation and biological self-assembly processes. NFGAIL and FGAIL are very good examples of short peptides, which can self-assemble into fibrillar structure.[54]

To understand the amyloid fibril formation better, further investigations were conducted to find the minimum peptide fragment which was responsible for amyloid fibrils formation. It was found that aromatic residues played critical roles in the process of amyloid formation. Diphenylalanine (FF) is the core recognition motif of the Alzheimer's β-amyloid polypeptide. FF leads the process of self-assembly in the molecule. In fact, dipeptide containing FF underwent self-assembly into nanotubes through a combination of π-π stacking and hydrogen bonding (Figure

20).[55] Larger peptides and conjugated organic molecules that contain this motif inhibited fibrils formation by Aβ.[56,57]

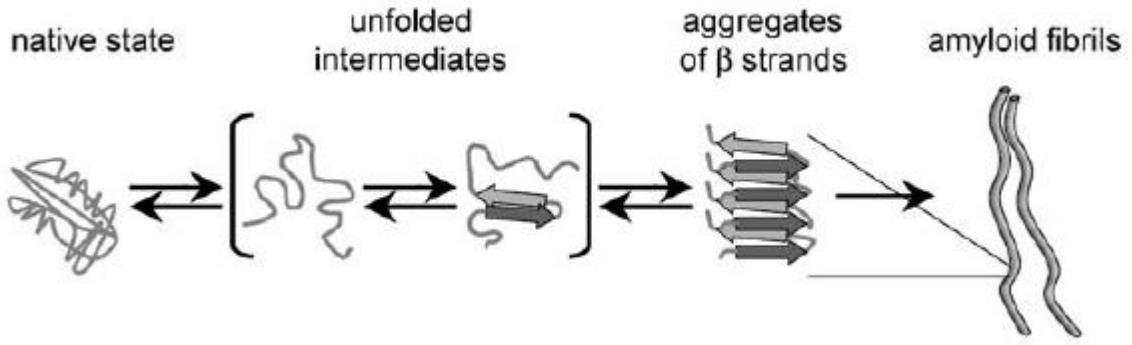

Figure 20. The formation of amyloid fibrils. Folded monomer undergoes a conformational transition into a b-sheet-rich state, usually through a partial unfolded state. Self-assembly of these intermediates into ladders of b strands results in the formation of ordered filaments that aggregate into the well-known amyloid fibrils. Reprinted with permission from ref. 55. Copyright 2013 Wiley Publishing Group.

These peptide nanotubes developed from diphenylalanine are significantly rigid and potentially useful in electrochemical biosensing.[58] Gazit et al. and Ulijn et al. found that 9-fluorenylmethoxycarbonyl (Fmoc) protected diphenyalanine (Fmoc-FF) self-assembled into nanofibrils in aqueous solution, which led to a hydrogel formation.[55-60] The rheological pattern of this hydrogel exhibited similarity to solid-like gels materials. This hydrogel was significantly stable at a wide range of temperatures and pH values including extreme acidic conditions. Recent molecular modeling studies showed that, peptides in this gel were aligned in an antiparallel β-sheet fashion and adjacent sheet like interlocked through lateral π-π interactions, which resulted to the formation of a cylindrical structure.[61] Modification of this dipeptide by *N*-terminal acetylation and

amidation of the *C*-terminal carboxyl led to the formation of nanotube structures of similar properties. These data indicated the key role of aromatic moieties in the generation of peptide nanotubes.[62]

Further extension of this study by Gazit et al. showed that diphenylglycine, a similar analogue of diphenylalanine and the simplest aromatic peptide, formed nanospheres. These nanostructures were stable under extreme chemical conditions. The introduction of a thiol group by incorporation of a cysteine residue into FF peptide modified the self-assembly properties of the resultant building blocks. Cysteine-diphenylalanine tripeptide self-assembled into spherical vesicles instead of nanotubes.[7]

2.6. Rod-Coil/Coiled coil Nanostructures

Rod-coil nanostructures have a chain of rod-like stiffness and flexible coil-like block. Like other supramolecular building blocks, rod-coil block molecules can be used to construct a variety of distinct nanostructures of controlled size and shape in some selective solvents. For aqueous self-assembly of this molecule, one part was designed to be hydrophilic, and another part was hydrophobic. For example, Holowka, et. al. reported the preparation of charged amphiphilic block copolypeptides that formed vesicles and micelles in water. They were synthesized a class of poly(L-lysine)-*b*-poly(l-leucine) block copolypeptides, K_xL_y, where $x = 20–80$ and $y =$ 10-30 amino acids (Figure 21).[63]

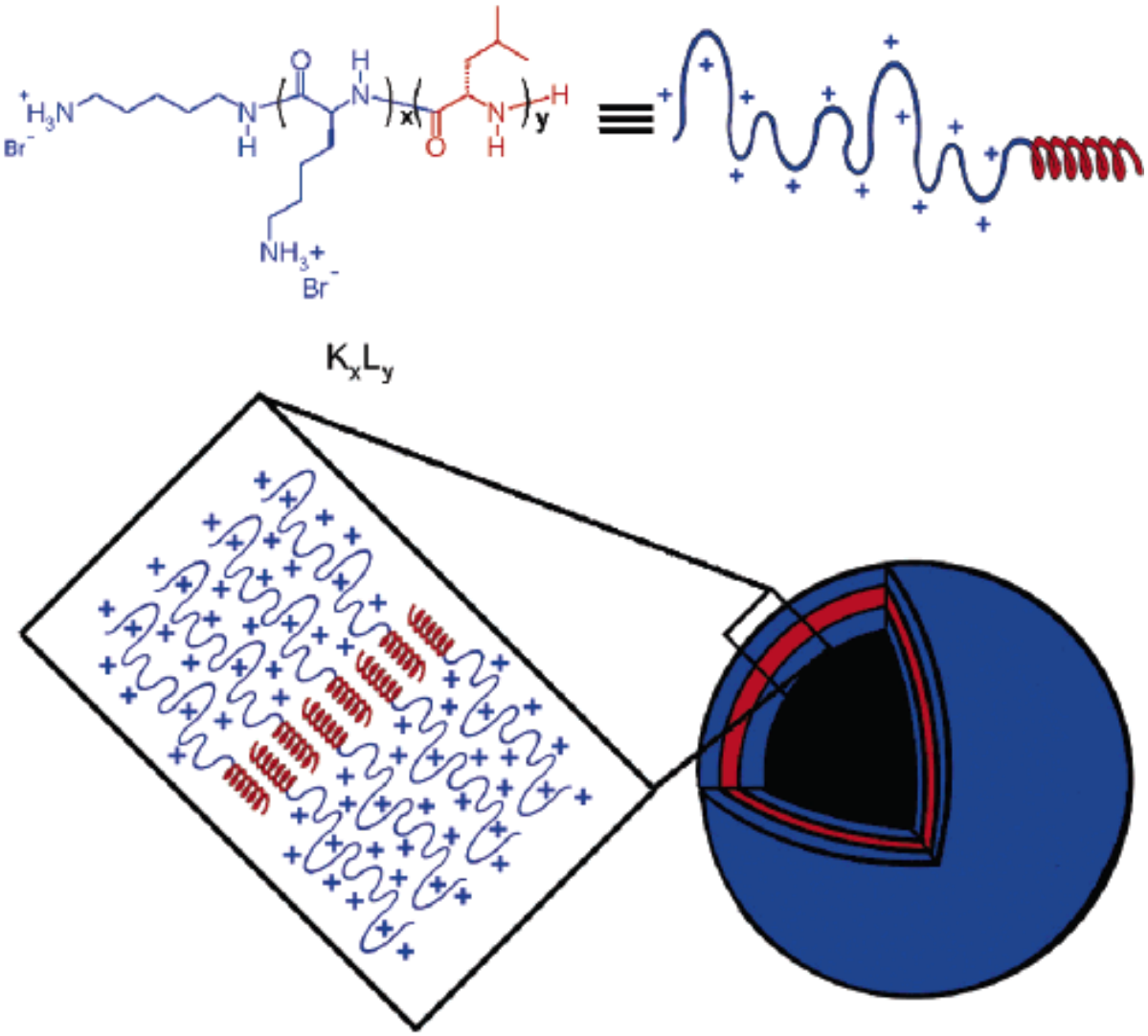

Figure 21. Schematic drawing showing proposed self-assembly of $K_{60}L_{20}$ into vesicles. Reprinted from ref. 63. Copyright 2013 American Chemical Society.

Lomander et al reported the hierarchical self-assembly of a coiled-coil peptide of 31 residues containing charged and hydrophobic residues.[64] The sequence is WGCIKQLEDKIEELLSKIY-HLENEIARLKKL. Internal cysteine has been used in the sequence to generate disulfide covalent bond between two separate peptide coiled-coils. Even though coiled-

coil peptide contained many charges, the secondary structure of the peptide in all pH ranges showed a typical α-helix with some variation of helical content. These findings suggested that the neutralization of the charged residues did not completely disrupt the secondary structure of the coiled-coil, mainly due to the hydrophobic interactions of two helices.

Coiled-coil peptides were reported to be an effective scaffold for creating new nanostructures. One such example is demonstrated by Ryadnov et al.[65] who designed a nanoreactor with multiple cavities by using self-assembled supramolecular dendrimers, which were termed as supradendrimers (SD) in two steps. The first step was the self-assembly of a single peptide sequence SD-1 (QEIARLEQEIARLEYEIARLE), which was based on a dimeric coiled coil also known as the leucine zipper. In folding state, SD-1 dimers were rigid rods. However, when self-assembly started and was sustained by the formation of hollow dendrimer cells, the rods extended into tightly packed noncovalent networks. TEM revealed very dense mesoscopic assemblies of a hexagonal paracrystalline phase, which proposed with the formation of a hierarchically ordered architecture of SD-1 supradendrimers.

Second step was to generate cavities in the dendrimer cells. To accomplish this, another complementary sequence SD-2 [Ac-(K(KIEALKOKIEALKYKIEALK- εAhx))$_3$ – am] where εAhx was ε-aminohexanoic acid, was assembled with SD-1, resulting a dimer SD-1,2 (Figure 22). Furthermore, to demonstrate the encapsulation ability of this dimer, a redox reaction was carried out, where boiling solution of silver nitrate was added into the dimer followed by the addition of sodium citrate as a reductant. This reaction led to the formation of silver nanoparticles having the size of the cavities, indicating nanoreactor nature of the dimer.

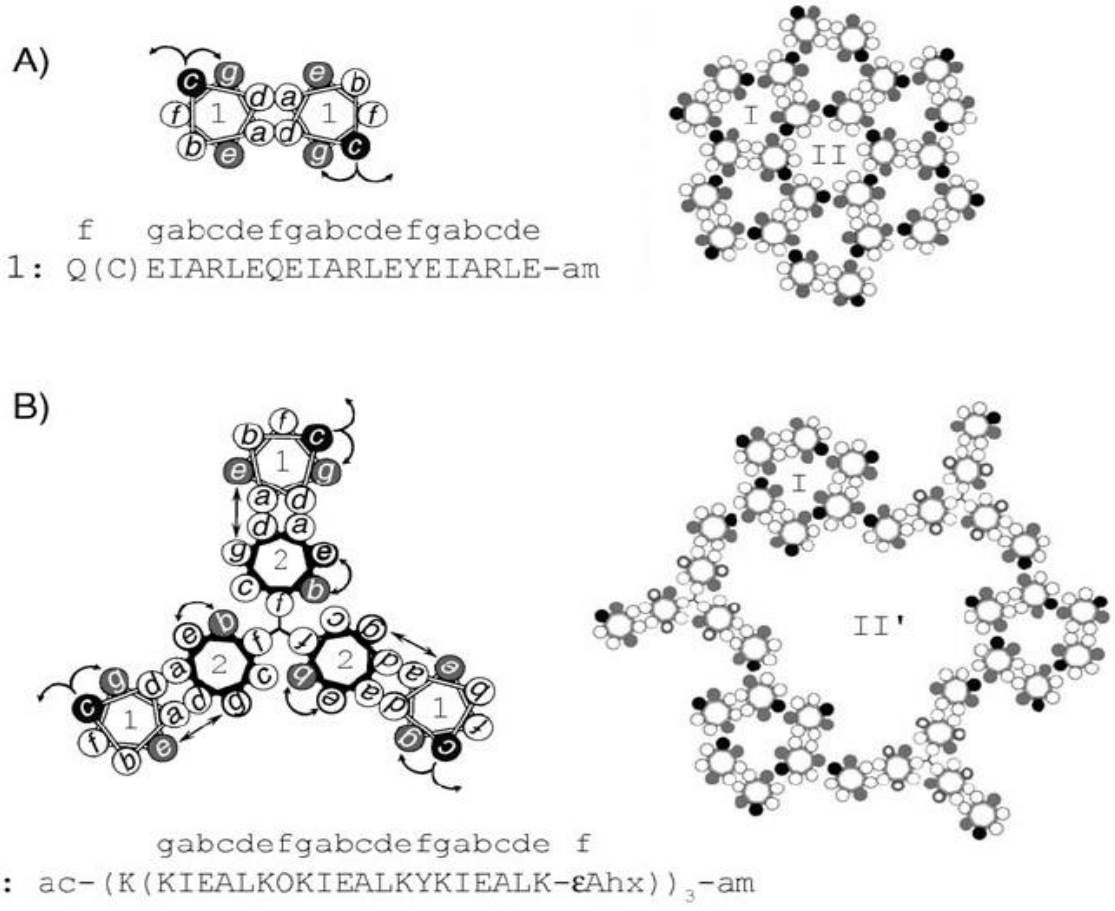

Figure 22. Schematic representation of the supradendrimer design. SD-1 (1) and SD-2 (2) peptide sequences are shown with the one-letter code and are simplified into helical wheels with 3.5 residues per turn. The sequences show heptad repeats characteristic of canonical coiled coils, commonly labeled a–g. Residues at sites a and d shape helix–helix interfaces. These are hydrophobic and made up of isoleucine and leucine, respectively, to ensure the formation of dimers. A) SD-1-type of electrostatic interactions, g–c–e': e' and g positions are occupied by glutamates that form salt bridges with arginine residues at c; g–c interactions are intrahelical, whereas c–e' are interhelical and are between two SD-1 copies of different dimers. Dimers trimerize (I) to give a noncovalent dendrimeric architecture, with a branching cell formed by six dimers (II). A single cysteine residue in the f position that replaces a glutamine is shown in

brackets. B) Mixed SD-1/SD-2 (SD-1,2)-type of electrostatic interactions, g–c–e'(1)/b–e, g–e'(2): intrahelical b–e interactions in 2 inhibit interhelical e–g' interactions; g–e' interactions contribute to the 1–2 interface. Because the width of a superhelix is approximately 2 nm, the diameter of an extended branching cell (II') is estimated to not exceed 4–6 nm. To form the supradendrimer II', each copy of SD-2 should be arranged with at least nine copies of SD-1 to round the equimolar SD-1,2 ratio to 10:1. SD-2 wheels are highlighted in black around an ac-KKK-am hub containing an e-aminohexanoic acid (eAhx) as spacer. The circles of helical wheels are black for arginines, gray for glutamates, and outlined in gray for lysines. Arrows represent salt bridges. Reprinted with permission from ref. 65. Copyright 2013 Wiley Publishing Group.

Table 1. Summary of peptides sequences and their self-assembled nanostructures incorporated in this review.

Peptide Sequence	Nanostructure	Reference
L-Phe-L-Phe (FF)	Nanotubes	8
cyclo[(D-Ala-Glu-D-Ala-Gln)$_2$]	Nanotubes	9
NH_2-(D)Naph-Cys-Tyr-(D)Trp-Lys-Val-Cys-Thr-$CONH_2$	Nanotubes	12
G_nD_2–OH (where n= 4, 6, 8, 10)	Nanotubes	14
Ac-V_6D-OH	Nanotubes and nanovesicles	15a
I_3K (Ac-I_3K-NH_2)	Nanotubes	15a
Ac-GAVILRR-NH_2	Nanosphere and nano-doughnut	16
Ac-$A_2V_2L_3WE_{2/7}$–OH	Nano-vesicles	18
A_6K	Nanotubes or nanofibrils	19
A_9K	Nanorods	20a
DiC_{16}-EQLESIINFEKLTWE	cylindrical micelles	20b
IKVAV	nanofiber	22
$A_{12}R_2$	twisted fibril	27b
Fmoc-βAH	Nanofibril	27c
C_{16}-βAH	Nanotape	27d
C_{16}-KTTKS	Fibrillar	27e
C_{16}-KTTKS and C_{16}-ETTES (mixed)	Nanotape	27h
C_{16}-W_3K (1 day)	Spherical micelles	27i
C_{16}-W_3K (13 days)	Worm-like micelles	27i
Polyethylene glycol- DGRFFF	Nanofibril	27l
Lauryl-VVAGE-Dopa-Am and Lauryl-KRSR-Am (KRSR-PA) (Mixture)	Nanofiber	27m
Palmitoyl-G$V_3A_3E_3$	Fibril	28
VEVE	Nanobelt	26,29
VVEE	Cylindrical nanofibers	26
FKFEFKFE	Nanofiber	30
C_3-symmetric peptide conjugate trigonal $(FKFEFKFE)_2$	Nanospheres	31
Ac-$(FKFE)_2$-NH_2	Amyloid fibril	32a
C_{12}-GAGAGAGY	Nanofiber	32b
Polyethylene glycol-$[(AG)_3EG]_n$	Fibril	33a
Polyethylene oxide-$[(Thr\text{-}Val)_5]$	Fibers	35
R-GRKKRRQRRRPPQGSGG-FKFEFKFEFKFE	Nanoribbon	36
Poly(L-lysine)-b-poly(L-leucine) and Poly(glutamic acid)-b-poly(L-leucine)	Vesicles	38
PGA-b-PLys	Vesicles	41

$P_{10}R_3$, P_{10}Tat	Vesicles	43,44
$[WR]_n$ (n=3-5)	Vesicle-like	45
$l(KW)_5$-AuNPs	Ball-shaped structures	47
$c[KW]_5$-AuNPs	Sponge-like agglomerates	47
PEpYLGLD-loaded $[WR]_4$	Large noncircular morphologies	48
Fmoc-FF	Nanofibrils	60
Diphenylglycine	Nanotubes and nanospheres	8
Cysteine-diphenylalanine tripeptide	Spherical vesicles	7
Poly(L-lysine)-*b*-poly(l-leucine)	Vesicles and micelles	63
WGCIKQLEDKIEELLSKIY-HLENEIARLKKL	Coiled coils	64
SD-1 (QEIARLEQEIARLEYEIARLE)	Coiled coils	65

3. Conclusions and Future outlook

Peptides are highly versatile structural building blocks and can generate supramolecular architectures, including sheets, spheres, fibres, tapes, and tubes. Self-assembled peptides are able to form numerous nanostructures through various types of interactions, such as electrostatic, hydrophobic, and hydrogen bonding. They can take advantage of diversity in the body of amino acid residues including positive or negative charge along with hydrophobic or hydrophilic properties. More studies are required in rational peptide design to investigate systematically the role of hydrophobicity, electrostatics, and size on pattern formation and to examine sequence effects on morphologies, and elucidate the fundamental physical interactions that drive their self-assembly. These investigations will assist us to determine the guiding principles in terms of roles of size, charge, and hydrophobicity for self-assembly into specific structures.

Several challenges including size control, undesired aggregation, pH stability and chemical and enzymatic stability need to overcome in design and functionalizing peptide nanostructures. The use of peptide nanostructures as drug delivery vehicles, imaging contrast agents and/or biosensors requires a good stability in the solution in question (e.g., buffer). For instance, Stupp and his group found that some PAs were unstable upon pH change.[24] When a dumbbell-shaped

hydrophobic core was added into the sequence, it showed enhanced stability.[25] However, extensive studies are required to evaluate the properties of peptide nanostructures upon the pH change. It was found that tryptophan containing cyclic peptides $[WR]_n$ (where n = 3-5) did not exhibit self-assembled nanostructures immediately, but in a long period of time (approximately 12 days).[45] This issue can be addressed by altering the hydrophobic–hydrophilic ratio in the peptide sequence. The control of the size of peptide nanostructures is very crucial in its applications such drug delivery systems and biosensors. Nanostructures of equivalent dimension are needed for the fabrication of biosensing platforms of similar characteristics. It is very challenging to control the size of the nanostructures during the synthesis due to the self-assembly process. To obtain the nanostructures of similar dimension, change in fabrication parameters or use of templates can be beneficial. The size distribution of self-assembled peptides can be controlled with external stimulus, such as pH, ionic strength, solvent, chemical additives, or temperature. Particle size, charge, and size distribution can be intelligently engineered to affect the stability of self-assembled structure and encapsulation properties. Because of the presence of hydrophobic groups in some peptides, aggregation could occur. An optimal balance of hydrophobicity and charge could generate self-assembled nanostructures in aqueous solution by intramolecular and/or intermolecular interactions minimizing aggregation through hydrophobic groups. In some cases, due to strong interactions some crude peptides aggregate and thus, difficult to purify. Effective synthetic strategies are needed to overcome this problem.

Second, self-assembled peptides have been studied in diverse applications ranging from imaging, biomineralization, tissue engineering, and drug delivery, due to their inherent biocompatibility and biodegradability. Designing self-assembled peptides has emerged as an effective tool in applications ranging from energy storage, tissue engineering, drug and gene

delivery, membrane protein stabilization, due to their inherent biocompatibility and biodegradability. A deep understanding of self-assembly by amphiphilic peptides through systematic design and study of unexplored peptide sequences is urgently required to develop the next generation of self-assembled peptides for various applications, such as encapsulating hydrophobic compounds. Based on the desired applications, different number and types of amino acids can be used. Moreover, they can be easily conjugated with antibodies, enzymes, quantum dots, and metal nanoparticles to enhance their stabilization and biocompatibility. Peptide nanomaterials as self-assembled structures continue to have potential applications as encapsulation and/or drug delivery tools. Although further investigations on self-assembled peptide nanoparticles are required, they have already been used for different applications including drug delivery, wound healing, tissue engineering, surfactants, and tissue repair. It is envisioned that the peptide nanostructures may be specifically used in tissue engineering (e.g., wound healing and nerve regeneration), drug delivery, imaging, and active targeting to disease-relevant cell types for the efficacious treatment of a variety of ailments, including cancer and neurodegenerative disorders. Nevertheless, the application of peptide nanostructures in the area of gene/oligonucleotide delivery has not been explored extensively. The intracellular delivery of such macromolecules in their active form remains a challenging task. To address this issue, rationally designed peptide-polymer conjugates with desired properties are needed to explore. Furthermore, the biocompatibility and immunogenicity of the self-assembled peptide biomaterials is needed to study completely for possible biomedical applications. The synthesis of a variety of self-assembled peptides has been previously reported, but a predictive understanding for rational design of peptide self-assembly is still lacking. Thus, there is an urgent need to study systematically alternative peptides for establishing the relationship between the morphology of self-assembled peptides with

their physicochemical properties (e.g., sequence, size, charge, and 3D structure of the monomer). There is also a need to further study alternative systems for the prediction of structure of self-assembled peptides based on their sequence and other physiochemical properties.

Acknowledgements

We thank the National Center for Research Resources, NIH, and Grant Number 1 P20 RR16457 for sponsoring the core facility.

References

1. J. M. Lehn, *Proc. Natl. Acad. Sci. USA*, 2002, **99**, 4763-4768.

2. G. M. Whitesides, J. P. Mathias, C. T. Set, *Science* 1991, ***254***, 1312-1319.

3. J. C. Sacchettini and J. W. Kelly, *Nat. Rev. Drug Discov.* 2002, **1**, 267-275.

4. a) Y. B. Lim, K. S. Moon, M. Lee, *Chem. Soc. Rev.* 2009, **38**, 925–934. b) R. V. Ulijn, A. M. Smith, *Chem. Soc. Rev.* 2008, **37**, 664–675.

5. a) M. Zelzer, R. V. Ulijn. *Chem. Soc. Rev.* 2010, **39**, 3351–3357. b) R. D. L. Rica, H. Matsui, *Chem. Soc. Rev.* 2010, **39**, 3499–3509.

6. a) E. Gazit, *Chem. Soc. Rev*. 2007, **36**, 1263-1269. b) X. Zhao, F. Pan, H. Xu, M. Yaseen, H. Shan, CA. Hauser, S. Zhang, and JR. Lu, *Chem. Soc. Rev*., 2010, **39**, 3480-3498. c) C. A. E. Hauser and S. G. Zhang, *Chem. Soc. Rev*., 2010, **39**, 2780-2790. d) I. W. Hamley, *Soft Matter*, 2011, **7**, 4122–4138.

7. C. R. Martin and P. Kohli, *Nat. Rev. Drug discovery*, 2003, **2**, 29-37.

8. M. Reches and E. Gazit, *Nano Lett.*, 2004, **4**, 581-585.

9. a) M. R. Ghadiri, J. R, Granja, R. A. Milligan, D. E. McRee, N. Khazanovich, *Nature* 1993, **366**, 324-327. (b) M. R. Ghadiri, J. R. Granja, L. K. Buehler, *Nature* 1994, **369**, 301-304.

10. J. D. Hartgerink J. R. Granja, R. A. Milligan and M. R. Ghadiri, *J. Am. Chem. Soc.* **1996**, ***118***, 43-50.

11. S. Fernandez-Lopez, H.-S. Kim, E. C. Choi, M. Delgado, J. R. Granja, A. Khasanov, K. Kraehenbuehl, G. Long, D. A.Weinberger, K. M. Wilcoxen, and M. R. Ghadiri, *Nature* **2001**, ***412***, 452-455.

12. C. Valery, M. Paternostre, B. Robert, T. Gulik-Krzywicki, T. Narayanan, J. Dedieu, G. Keller, M. Torres, R. Cherif-Cheikh, P. Calvo, and F. Artzner, *Proc. Natl. Acad. Sci*. *U. S. A*, 2003, **100**, 10258-10262.

13. H. Cui, M. J. Webber, and S. I. Stupp, *Biopolymers* 2010, **94**, 1-18.

14. a) S. Santoso, W. Hwang, H. Hartman, and S. Zhang, *Nano Lett* 2002, **2**, 687-691. (b) X. Zhao and S. Zhang, *Chem. Soc. Rev.* 2006, **35**, 1105-1110.

15. a) S. Bucak, C. Cenker, I. Nasir, U. Olsson, and M. Zackrisson, *Langmuir* 2009, **25**, 4262-4265. b) D. A. Middleton, J. Madine, V. Castelletto, and I.W. Hamley, *Angew. Chem. Int. Ed*. 2013, **52**, 10537 –10540. b) X. Zhao, Y. Nagai, P. J. Reeves, P. Kiley, H.G. Khorana, and S. Zhang, *Proc. Natl. Acad. Sci. USA*, 2006, **103**, 17707-17712.

16. U. Khoe, Y. Yang, and S. Zhang, *Langmuir* 2009, **25**, 4111-4114.

17. Y. Yang, U. Khoe, X. Wang, H. Akihiro, H. Yokoi and S. Zhang, *Nano Today*, *2009*, **4**, 193-210.

18. A. J. van-Hell, C. I. C. A. Costa, F. M. Flesch, M. Sutter, W. Jiskoot, D. J. A. Crommelin, W. E. Hennink, and E. Mastrobattista, *Biomacromolecules*, 2007, **8**, 2753-2761.

19. H. Xu, J. Wang, S. Han, J. Wang, D. Yu, H. Zhang, D. Xia, X. Zhao, T. A. Waigh, and J. R. Lu, *Langmuir*, 2009, **25**, 4115-4123.

20. a) J. Wang, S. Han, G. Meng, H. Xu, D. Xia, X. Zhao, R. Schweins, and J. R. Lu, *Soft Matter*, 2009, **5**, 3870-3878. b) M. Black, A. Trent, Y. Kostenko, J.S. Lee, C. Olive, and M. Tirrell, *Adv. Mater*. 2012, **24**, 3845–3849.

21. H. A. Behanna, J. J. Donners, A. C. Gordon, and S. I. Stupp, *J. Am. Chem. Soc*. 2005, **127**, 1193-1200.

22. G. A. Silva, C. Czeisler, K. L. Niece, E. beniash, D. A. Harrington, J. A. Kessler and S. I. Stupp, *Science*, 2004, **303**, 1352-1355.

23. J. D. Tovar, R. C. Claussen and S. I. Stupp, *J. Am. Chem. Soc.* 2005, **127**, 7337-7345.

24. J. D. Hartgerink, E. Beniash, S. I. Stupp, *Science* 2001, **294**, 1684-1688.

25. S. R. Bull, L. C. Palmer, N. J. Fry, M. A. Greenfield, B. W. Messmore, T. J. Meade and S. I. Stupp, *J. Am. Chem. Soc*, 2008, **130**, 2742-2743.

26. H. Cui, T. Muraoka, A. G. Cheetham and S. I. Stupp, *Nano Lett.*, 2009, **9**, 945-951.

27. a) H. K. Lee, S. Soukasene, H. Z. Jiang, S. M. Zhang, W. C. Feng and S. I. Stupp, *Soft Matter* **2008**, 4, 962-964. b) I.W. Hamley, A. Dehsorkhi, V. Castelletto, J. Seitsonen, J. Ruokolainen, and H. Iatrou, *Soft Matter*, 2013, **9**, 4794-4801. c) V. Castelletto, G. Cheng, B. W. Greenland, and I. W. Hamley, *Langmuir*, 2011, **27**, 2980–2988). d) V. Castelletto, G. Cheng, C. Stain, C. J. Connon, and I. W. Hamley, *Langmuir*, 2012, **28**, 11599−11608. e) V. Castelletto, I.W. Hamley, J. Perez, L. Abezgauz, and D. Danino, *Chem. Commun.*, 2010, **46**, 9185–9187. f) J. F. Miravet, B. Escuder, M. Dolores Segarra-Maset, M. Tena-Solsona, I. W. Hamley, A. Dehsorkhi, and V. Castelletto, *Soft Matter*, 2013, **9**, 3558-3564. g) A. Dehsorkhi, V. Castelletto, I. W. Hamley, J. Adamcik, and R. Mezzenga, *Soft Matter*, 2013, **9**, 6033-6036. h) I.W. Hamley,

A. Dehsorkhi, and V. Castelletto, *Langmuir,* 2013, **29**, 5050−5059. i) T. Shimada, S. Lee, F.S. Bates, A. Hotta, and M. Tirrell, *J. Phys. Chem. B* 2009**, 113**, 13711–13714. j) S. Bulut, T.S. Erkal, S. Toksoz, A. B. Tekinay, T. Tekinay, and M.O. Guler, *Biomacromolecules* 2011, **12**, 3007–3014. k) I.W. Hamley, A. Dehsorkhi, P. Jauregi, J. Seitsonen, J. Ruokolainen, F. Coutte, G., Chataigné, and P. Jacques, *Soft Matter*, 2013, **9**, 9572-9578. l) V. Castelletto, R. J. Gouveia, Ch. J. Connon, and I.W. Hamley, *European Polym. J.* 2013, **49**, 2961–2967. m) H. Ceylan, S. Kocabey, A. B. Tekinay, and M. O. Guler, *Soft Matter*, 2012, **8**, 3929–3937.

28. T. Muraoka, H. Cui and S. I. Stupp, *J. Am. Chem. Soc*, 2008, **130**, 2946-2947.
29. H. Dong, S. E. Paramonov, L. Aulisa, E. L. Bakota, J. D. Hartgerink, *J. Am. Chem. Soc*, 2007, **129**, 12468-12472.
30. D. M. Marini, W. Hwang, D. A. Lauffenburger, S. Zhang, and R. D. Kamm. *Nano Lett.* 2002, **2**, 295-299.
31. K. Matsuura, K. Murasato and N. Kimizuka, *J. Am. Chem. Soc*., 2005, **127**, 10148-10149.
32. a) C. J. Bowerman and B. L. Nilsson, *J. Am. Chem. Soc*., 2010, **132**, 9526-9527. b) J. Zhang, R. Hao, L. Huang, J. Yao, X. Chen, Z. Shao, *Chem. Commun.,* 2011, **47**, 10296–10298. c) J. Shu, B. Panganiban, and T. Xu, *Annu. Rev. Phys. Chem.* 2013. 64, 631-657. d) B. Siddique and J. Duhamel, *Langmuir*, 2011, **27**, 6639−6650.
33. a) J. M. Smeenk, M. B. J.Otten, J. Thies, D. A. Tirrel, H. G. Stunnenberg and J. C. M. van Hest, *Angew. Chem. Int. Ed*, 2005, **44**, 1968-1971. b) J. T. Meijer, M. J. A. G. Henckens, I. J. Minten, D. W. P. M. Löwik, and J. C. M. van Hest, *Soft Matter*, 2007, **3**, 1135–1137.
34. D. Eckhardt, M. Groenewolt, E. Krause, H. G. Borner, *Chem. Commun*, 2005, 2814-2816.
35. J. Hentschel, E. Krause and H. G. Borner, *J. Am. Chem. Soc*., 2006, **128**, 7722-7723.
36. Y. B. Lim, E. Lee and M. Lee, *Angew. Chem. Int. Ed.*, 2007, **46**, 3475-3478.

37. S. Futaki, *Adv. Drug Delivery Rev.*, 2005, **57**, 547-548.

38. E. G. Bellomo, M. D. Wyrsta, L. Pakstis, D.J. Pochan and T. J. Deming, *Nat. Mater.*, 2004, **3**, 244-248.

39. E. P. Holowka, D. J. Pochan, and T. J. Deming, *J. Am. Chem. Soc*, 2005, **127**, 12423-12428.

40. E. P. Holowka, V. Z. Sun, D. T. Kamei and T. J. Deming, *Nat. Mater*, 2007, **6**, 52-57.

41. J. Rodriguez-Hernandez and S. Lecommandoux, *J. Am. Chem. Soc*, 2005, **127**, 2026-2027.

42. M. R. Dreher, A. J. Simnick, K. Fischer, R. J. Smith, A. Patel, M. Schmidt and A. Chilkoti, *J. Am. Chem. Soc*, 2008, **130**, 687-694.

43. Y.–R. Yoon, Y. –b, Lim, E. Lee and M. Lee, *Chem. Commun.*, 2008, 1892-1894.

44. Y.–b. Lim, E. Lee and M. Lee, *Angew. Chem. Int. Ed.*, 2007, **46**, 9011-9014.

45. D. Mandal, R. Tiwari, A. Nasrolahi Shirazi, D. Oh, G. Ye, A. Banerjee, A. Yadav, and K. Parang, *Soft Matter*, 2013, **9**, 9465-9475.

46. A. Nasrolahi Shirazi, D. Mandal, R. K. Tiwari, L. Guo, W. Lu, and K. Parang, *Mol. Pharm.* 2013, **10**, 500–511.

47. A. Nasrolahi Shirazi, R. K. Tiwari, D. Oh, B. Sullivan, K. McCaffrey, D. Mandal, and K. Parang, *Mol. Pharm.* 2013, **10**, 3137–3151.

48. A. Nasrolahi Shirazi, R. K. Tiwari, D. Oh, A. Baerjee, A. Yadav, and K. Parang, *Mol. Pharm.* 2013, **10**, 2008–2020.

49. D. Mandal, A. Nasrolahi Shirazi, K. Parang, *Angew. Chem. Int. Ed*. 2011, **50**, 9633–9637.

50. A. Nasrolahi Shirazi, D. Mandal, R. K. Tiwari, L. Guo, W. Lu, K. Parang, *Mol. Pharm.* 2013, **10**, 488–499.

51. R. Nelson, M. R. Sawaya, M. Balbirnie, A. O. Madsen, C. Riekel, R. Grothe and D. Eisenberg, *Nature*, 2005, **435**, 773-778.

52. C. G. Glabe, *Neurobiology of Aging*, 2006, **27**, 570–575.

53. M. Reches, Y. Porat E. Gazit, *J. Biol. Chem*., 2002, **277**, 35475–35480.

54. K. Tenidis, M. Waldner, J. Bernhagen, W. Fischle, M. Bergmann, M. Weber, M. Merkle, W. Voelter, H. Brunner, and A. Kapurniotu, *J. Mol. Biol*., 2000, **295**, 1055-1071.

55. I. Cherny, E. Gazit, *Angew. Chem. Int. Ed*., 2008, **47**, 4062-4069.

56. M.A. Findeis, G. M. Musso, C.C. Arico-Muendel, H. W. Benjamin, A. M. Hundal, J.J. Lee, J. Chin, M. Kelley, J. Wakefield, N.J. Hayward, S.M. Molineaux, *Biochemistry*, 1999, **38**, 6791-6800.

57. C. Soto, E.M. Sigurdsson, L. Morelli, R.A. Kumar, E.M. Castano, B. Frangione, *Nature Med.*, 1998, **4**, 822-826

58. M. Yemini, M. Reches, J. Rishpon and E. Gazit, *Nano Lett.*, 2005, **5**, 183-186.

59. V. Jayawarna, M. Ali, T. A. Jowitt, A. E. Miller, A. Saiani, J. E. Gough and R. V. Ulijn, *Adv. Mater*, 2006, **18**, 611-614.

60. A. Mahler, M. Reches, M. Rechter, S. Cohen and E. Gazit, *Adv. Mater*, 2006, **18**, 1365-1370.

61. A. M. Smith, R. J. Williams, C. tang, P. Coppo, R. F. Collins, M. L. Turner, A. Saiani and R. V. Ulijn, *Adv. Mater*, 2008, **20**, 37-41.

62. M. Reches and E. Gazit, *Isr. J. Chem*, 2005, **45**, 363-371.

63. E. P. Holowka, D. J. Pochan, T.J. Deming, *J. Amer. Chem. Soc.*, 2005, **127**, 12423-12428.

64. A. Lomander, W. Hwang, and S. Zhang, *Nano Lett.*, 2005, **5**, 1255-1260.

65. M. G. Ryadnov, *Angew. Chem. Int. Ed*, 2007, **46**, 969-972.